Strontium Isotope Investigation of Ungulate Movement Patterns on the Pleistocene Paleo-Agulhas Plain of the Greater Cape Floristic Region, South Africa

Sandi R. Copeland[x]

Hayley C. Cawthra[x]

Erich C. Fisher[x]

Julia A. Lee-Thorp[f]

Richard M. Cowling[x]

Petrus J. le Roux[x]

Jamie Hodgkins[x]

Curtis W. Marean[x]

[a]Environmental Stewardship Group, Los Alamos National Laboratory, MS J978, Los Alamos, NM 87544, USA

[b]Department of Anthropology, University of Colorado Boulder, Campus Box 233 UCB, Boulder, CO 80309-0233, USA

[c]Geophysics Competency, Council for Geoscience, PO Box 572, Bellville, 7535, South Africa

[d]Centre for Coastal Palaeoscience, Nelson Mandela Metropolitan University, PO Box 77000, Port Elizabeth, 6031, South Africa

[e]Institute of Human Origins, School of Human Evolution and Social Change, Arizona State University, Tempe, AZ 85287-2402, USA

[f]Research Laboratory for Archaeology, University of Oxford, Oxford, OX1 3QY, UK

[g]Evolutionary Studies Institute, University of the Witwatersrand, Private Bag 3, Wits 2050, South Africa

[h]Department of Geological Sciences, University of Cape Town, South Africa

[i]Department of Anthropology, University of Colorado Denver, P.O. Box 173364, Denver, CO 80217-3364, USA

Abstract

Middle Stone Age sites located within the Greater Cape Floristic Region on the South African southern coast have material culture with early evidence for key modern human behaviors such as projectile weaponry, large animal hunting, and symbolic behavior. In order to interpret how and why these changes evolved, it is necessary to understand their ecological context as it has direct relevance to foraging behavior. During periods of lowered sea level, a largely flat and vast expanse of land existed south of the modern coastline, but it is now submerged by higher sea levels. This exposed area, the Paleo-Agulhas Plain, likely created an ecological context unlike anything in the region today, as evidenced by fossil assemblages dominated by migratory ungulates. One hypothesis is that the Paleo-Agulhas Plain supported a migration ecosystem of large grazers driven by summer rainfall, producing palatable forage during summer in the east, and winter rainfall, producing palatable forage during winter in the west. Alternatively, ungulates may have been moving from the coastal plain in the south to the interior north of the Cape Fold Mountains, as observed for elephants in historic times.

In this study, we assess ungulate movement patterns with inter- and intra-tooth enamel samples for strontium isotopes in fossil fauna from Pinnacle Point sites PP13B and PP30. To accomplish our goals we created a bioavailable $^{87}Sr/^{86}Sr$ isoscape for the region by collecting plants at 171 sampling sites and developing a geospatial model. The strontium isotope results indicate that ungulates spent most of their time on the Paleo-Agulhas Plain and avoided dissected plain, foothill, and mountain habitats located more than about 15 km north of the modern coastline. The results clearly exclude a north-south

(coastal-interior) movement or migration pattern, and cannot falsify the east-west movements hypothesized in the south coast migration ecosystem hypothesis.

1. INTRODUCTION

A series of South African Middle Stone Age (MSA) sites dating from ~160-50 ka provide evidence that has revised our understanding of the timing and pace of behaviors considered indicative of modern humans. Many of these sites are on the coast of the Greater Cape Floristic Region (GCFR) (Figure 1), an area with Mediterranean climate and unique vegetation that is a plant biodiversity hotspot and center of endemism (Allsopp et al., 2014), but which is currently depauperate in large ungulates. The locality of our study is Pinnacle Point, which is within the GCFR (Marean et al., 2014) and contains sites with the earliest evidence for stone tool microlithic technology ~71 ka (Brown et al., 2012), heat-treated stone tool production ~160 ka (Brown et al., 2009), and early evidence for humans using coastal resources ~160 ka (Marean, 2014; Marean et al., 2007). Genetic and fossil evidence suggest that the modern human lineage appears by at least ~200-160 ka (Clark et al., 2003; Gonder et al., 2007; McDougall et al., 2005), and of the handful of sites in Africa that are numerically dated to this time interval, only two are in South Africa (Border Cave and Pinnacle Point 13B) and one of these is in the GCFR (Pinnacle Point 13B) (Marean et al., 2007). It has been hypothesized (Marean, 2011; 2010) that the origin lineage of the indigenous inhabitants of the southern African sub-region, identified by genetic evidence (Henn et al., 2011; Pickrell et al., 2012; Schlebusch et al., 2012), found refuge along the southern shorelines during the long glacial cycle of Marine Isotope Stage (MIS) 6 (~195-125 ka) (Petit et al., 1999). For these

reasons there is an ongoing multi-disciplinary effort to develop a detailed reconstruction of the paleoecological context of this region during the origins of modern humans (Franklin et al., 2015; Marean et al., 2014; 2015).

Klein (1983) noted that the faunal changes in the GCFR from the Pleistocene to the Holocene were greater than in any other African region with the possible exception of the Maghreb. Archaeological sequences dating to the Holocene –when the current sea levels and patterns of climate were rather stable and similar to modern – document a terrestrial fauna dominated by small-bodied residential species such as grysbok, hyrax, dune mole rats, and tortoises (Marean et al., 2014). In contrast, the Pleistocene MSA and Later Stone Age (LSA) sequences found along the South African coast were dominated by large and medium-sized ungulates (both extinct and extant) that are typical of open-habitat migratory ecosystems (Klein, 1983). An early microlithic stone tool technology found at Pinnacle Point is further hypothesized to have been a component of projectile weapons designed to hunt large mammals safely and effectively (Brown et al., 2012). Open-habitat species that were present in the Pinnacle Point MSA levels (Rector and Reed, 2010) include black wildebeest (*Connochaetes gnou*), hartebeest (*Alcelaphus buselaphus*), springbok (*Antidorcas marsupialis*), zebra (*Equus* cf. *quagga*), and the extinct giant buffalo (*Syncerus antiquus*). Prior to fencing and habitat destruction, some of these species formed migratory associations of millions of animals in the interior well north of the south coast in the South African Highveld and Karoo that did not penetrate into the GCFR (Cronwright-Schreiner, 1925; Estes 1991).

The dramatic faunal change between glacial and interglacial climates may seem surprising given that the GCFR was subject to rather muted climatic change through the

Pleistocene (Chase and Meadows, 2007; Marean et al., 2014). Off the coast of the GCFR is the gradually descending and low-relief Agulhas bank, and during periods of lowered sea level varying portions of this landmass were exposed (Van Andel, 1989). A computer model of the changing character of this "Paleo-Agulhas Plain" shows that it was relatively flat, and during peak sea level regressions exposed about 80,000 km^2 of land (Figure 2) – equivalent to the size of Ireland (Fisher et al., 2010). The plain is hypothesized to have been a refuge for humans during glacial phases (Compton, 2011). Marine geophysics studies provide further details and document the presence of broad floodplains (Cawthra et al., 2015). Thus, while changes in climate may have been relatively subtle between the Pleistocene and Holocene, changes in the landmass of the GCFR were huge and probably drove ecological change in the region (Marean et al., 2014). Furthermore, the character of the coastal foreland differed both geomorphologically and edaphically. The modern/Holocene coastal foreland is composed of highly dissected Paleogene rocks, whereas the variably exposed Paleo-Agulhas Plain of the Pleistocene was dominated by Cretaceous mudstones proximally and marine sediments distally (Cawthra et al., 2015). The soils derived from Paleo-Agulhas Plain substrata would have been considerably more fertile than those derived from the ancient rocks of its hinterland.

The current GCFR does not support the large grazers that were common in the Pleistocene, so what differences might account for this? Within the GCFR (Figure 1) there is a gradient of increasing summer rain from west to east along the south coast. West of Cape Agulhas is the winter rainfall zone in which more than 66% of mean annual precipitation falls between April-September (Chase and Meadows, 2007). Between Cape

Agulhas and Mossel Bay, rainfall is bimodal with peaks in spring and autumn and with reliable winter but unreliable summer rain. East of Mossel Bay, rainfall is similarly bimodal but with increasingly reliable summer component (Bradshaw and Cowling, 2014). Further east and north, beyond the GCFR, is the summer rainfall zone (Schulze, 1972). Carbon and oxygen isotope evidence in speleothems from Pinnacle Point (Bar-Matthews et al., 2010) and carbon isotope evidence from Nelson Bay Cave fauna (Sealy, 1996) suggest that this east-west rainfall gradient was a persistent feature during the Late Pleistocene. Furthermore, the presence of the GCFR itself indicates the persistence of this flora that is typically low in grasses over great time depth.

During lower sea levels, the large, flat Paleo-Agulhas Plain may have provided the environmental conditions for a greater grassy component on the landscape. The grasses could have occurred in extensive grasslands, but it is also possible that grasses grew as a component of grassy shrublands, or that grasses were concentrated in localized habitats such as seasonally waterlogged areas, as is found in the eastern GCFR today (Cowling and Potts, 2015). Bimodal rains falling on the easterly portion of the GCFR may have produced fresh grass during the warm season whereas the winter rains in the west produced expanses of fresh grass during the winter. A speleothem record dating from 90-53 ka has been interpreted as indicating an increase in the amount or proportion of summer rain during MIS 4 in the Pinnacle Point region (Bar-Matthews et al., 2010). Such changes in the distribution of summer and winter rain in the past may have had significant impacts on the suitability of the region for an east-west migratory system.

These rainfall conditions were hypothesized to provide the push and pull for a classic migration ecosystem on the Paleo-Agulhas Plain in the Pleistocene whereby

145 animals moved east and then west to take advantage of summer and winter rains and
146 green grass, respectively (Marean, 2010; Marean et al., 2014). The mortality patterns of
147 fossil specimens of the blue antelope *Hippotragus leucophaeus* from sites along the south
148 coast are consistent with an east-west migration (Faith and Thompson, 2013). An
149 alternative hypothesis is that animals moved along a north-south axis, migrating from the
150 coastal plains, through mountain passes of the Outeniqua Mountains, and into the Little
151 Karoo intermontane basin. Historical observations that elephants followed such a path
152 (Skead, 2011) are consistent with this hypothesis. The rapid rise of sea levels in the early
153 Holocene submerged the Paleo-Agulhas Plain, and this may have been responsible for the
154 regional extinction of a variety of ungulates at the Pleistocene/Holocene boundary
155 (Marean, 2010; Marean et al., 2014).

156 In this study, we investigate animal movement patterns through the comparison of
157 strontium ($^{87}Sr/^{86}Sr$) isotopes serially measured from fossil mammal teeth from the
158 Pinnacle Point sites PP13B and PP30. Since the distribution of bioavailable $^{87}Sr/^{86}Sr$
159 across the GCFR has not been previously well documented, we develop an empirically
160 grounded and robust strontium isoscape that includes a predictive geospatial model
161 developed in GIS. We use the strontium isoscape to infer movement patterns of fossil
162 animals from the sampled sites.

163

164 **2. BACKGROUND**

165 ***2.1 Climate and Environment***

166 The south coast of South Africa lies at the confluence of two oceans (Atlantic and
167 Indian) and two major oceanic systems - the cold Benguela Upwelling on the west coast

and the warm Agulhas Current flowing down the east coast (Lutjeharms, 2006; Lutjeharms et al., 2001). There is an east-west gradient in plant carbon isotopes, with C_3 grasses giving way to proportionally more C_4 grass representation in the bimodal rainfall areas, and finally domination of C_4 grasses in the eastern summer rainfall areas (Cowling, 1983; Vogel et al., 1978). The present western, winter rainfall vegetation is not rich in grasses, but those that are present are mainly C_3. The vegetation in the eastern, summer rainfall zone is both richer in grasses and those present are largely C_4. Changes in the distribution of these rainfall and grass photosynthetic systems during portions of the late Pleistocene are reflected in the $\delta^{13}C$ of speleothems from Crevice Cave at Pinnacle Point (Bar-Matthews et al., 2010).

The GCFR is a Mediterranean vegetation that has one of the world's highest frequencies of endemic plants (69%) and is a region of megadiversity (Cowling and Lombard, 2002; Cowling et al., 2009; Goldblatt and Manning, 2002) and a globally-recognized biodiversity hotspot (Myers et al., 2000). The winter rainfall zone is thought to be the long-term stable core of the GCFR, with plant diversity and endemism declining from west to east (Cowling and Lombard, 2002).

The GCFR is composed of several biomes (Bergh et al. 2014). Fynbos forms the largest component, and is dominated by small-leafed evergreen shrubs and rushes (restios). It is typically found on nutrient-poor soils on leached quartzites and calcareous rocks, and fire is a key component of its regeneration. Thicket is found in areas protected from fire, and is dominated by evergreen shrubs and trees of tropical affinity; some forms comprise thicket clumps in a matrix of low, grassy shrubland (Vlok et al., 2003). Renosterveld, a grassy shrubland, is typically found on nutrient-rich soils (often on shales

of the Bokkeveld Group). Renosterveld has been largely transformed for agriculture, and has been suggested as a potential vegetation type that supported large-bodied grazing species in pre-colonial times (Boshoff and Kerley, 2001; Boshoff et al., 2001). It is possible that the large numbers of grazing species in the Pleistocene could be explained at least partially by these species living in Renosterveld. However, if that were true, then prehistoric faunal assemblages from the Holocene should preserve these taxa, and they do not. Holocene faunal assemblages are overwhelmingly dominated by taxa typical of the current GCFR and lack the Pleistocene grazing communities (Marean et al., 2014).

2.2 Geology

Rocks of different types and ages are often distinct in strontium isotope ratios ($^{87}Sr/^{86}Sr$), therefore we provide a review of the geology of the region. The geological history of the South Coast spans the last 700 Myr from the Neoproterozoic sequences to recent unconsolidated beach and dune sediments flanking the modern shoreline. The oldest South Coast 'basement' rocks comprise the Malmesbury, Kaaimans, and Cango Caves Groups and the Cape Granite Suite (~650 – 510 Ma), related to Pan African orogenesis during the formation of Gondwana (Rozendaal et al., 1999; Johnson et al., 2006; Milani and de Wit, 2008). Overlying deposits of the Cape Supergroup form a 6-10 km thick siliciclastic sequence, divided into the Table Mountain, Bokkeveld and Witteberg Groups (Thamm and Johnson, 2006). The Cape Orogeny (~278 – 230 Ma; Newton et al., 2006) resulted in the formation of the Cape Fold Belt. The fragmentation of Gondwana in the South Coast region and the opening of the South Atlantic commenced in the Early Cretaceous (~136 Ma) (Martin and Hartnady, 1986).

Compressional Cape Fold Belt faults were reactivated and the newly created accommodation space in basins was filled with clastic sediments of the Uitenhage Group (~145 – 130 Ma) (Paton et al., 2006). Offshore, arcuate normal faults bounded several graben and half graben structures that became the depocenters for terrigenous sediment sourced from the onshore areas (Broad et al., 2006; Tinker et al., 2008). Neogene and Quaternary aged Bredasdorp Group sediments are dominant along the southern coastal plain and include marine calcarenites (De Hoopvlei Formation), calcified aeolianites (Wankoe Formation), and aeolianites (Waenhuiskrans Formation) (Malan, 1990).

The southern coastal plain of South Africa extends south of the Langeberg–Outeniqua ranges (part of the Cape Fold Belt) from Bot River to Port Elizabeth. The continuity of the southern Cape coast from Port Elizabeth in the east to Cape Agulhas in the west is broken by a series of logarithmic spiral bays, linked to deformation associated with Gondwana break-up (Hälbich, 1983; Watkeys, 2006). The bedrock lithology of pre-Cenozoic strata along the south coast is highly variable, creating variation in geomorphic expression (Roberts et al., 2013).

Pinnacle Point caves and rockshelters, including PP13B, are formed in the sandstone of the Skurweberg Formation (part of the Table Mountain Group) capped by various Bredasdorp marine sediments (dunes, aeolianites, calcarenites, and calcretes) (Bar-Matthews et al., 2010; Karkanas and Goldberg, 2010). PP30 is a cave formed in the calcrete overlying the Table Mountain Group sandstone. The Paleo-Agulhas Plain now submerged off the coast includes Cretaceous Uitenhage lithologies and Mio-Pliocene limestones, cemented phosphatic rocks and ferricretes, such as the Cape St. Blaize, Cape

St. Francis, and Agulhas Formations (Figure 2) (Dingle et al., 1983; Parker and Siesser, 1972; Rogers, 1971a; 1971b).

These differences in the ages and composition of the rocks across the South Coast suggest that some should differ substantially in $^{87}Sr/^{86}Sr$ values. Previous studies that have measured $^{87}Sr/^{86}Sr$ in fauna, plants, soils, water, and rock from the GCFR (Table S1 and references therein) support this contention. For example, animals living on the Malmesbury shales in the Western Cape had $^{87}Sr/^{86}Sr$ of around 0.718 (Sealy et al., 1991), while rodents living on Bredasdorp sediments along the south coast have $^{87}Sr/^{86}Sr$ of about 0.709 (Radloff et al., 2010). This offers the possibility that strontium isotope analyses of fossil animal tissues might help resolve animal movement patterns.

2.3 Serial-Sampling of Teeth for Isotopic Analysis

Strontium isotopes have been shown to provide useful evidence for human mobility and animal movements because strontium becomes incorporated into growing tooth enamel, and does not alter after the tooth becomes fully mineralized (e.g., Ericson, 1985; Price et al., 1994; Gage et al., 1989). "Bioavailable $^{87}Sr/^{86}Sr$" that is found within the food chain derives from a combination of bedrock, soil, water, and/or atmospheric sources, and varies across landscapes. Mammalian molars grow from the apex of the tooth crown toward the neck over several months or years, incorporating the isotope ratios of the body pool into the enamel mineral lattice structure (Balasse, 2002; Passey and Cerling, 2002; Zazzo and Balasse, 2005).

There are limitations to the precision of intra-tooth isotope analysis due to attenuation of isotope values during incorporation into enamel, issues arising from

sampling methods, and varying or unknown rates of tooth growth and mineralization (Balasse, 2002). Although the tooth structure is formed in a generally sequential manner from apex to neck, there are successive waves of lattice formation and mineralization that occur at different rates across the three-dimensional tooth (Balasse, 2002; Hoppe et al., 2004; Zazzo et al., 2010). Furthermore, strontium may spend time in the body pool before it becomes incorporated into the animal's tissues (Montgomery et al., 2010).

Nonetheless, intra-tooth and inter-tooth $^{87}Sr/^{86}Sr$ values have been used with success, for example, to trace the movements of modern caribou in Alaska (Britton et al., 2009), mastodons in late Pleistocene North America (Hoppe and Koch, 2007) , and reindeer, bison, horse, and red deer in prehistoric Europe (Britton et al., 2011; Julien et al., 2012; Pellegrini et al., 2008; Price et al., 2015). In one prior study in the Western Cape of South Africa, strontium isotopes from archaeological sheep suggested annual movement of the animals from the coastal to inland areas (Balasse et al., 2002). If the fossil animals from Pinnacle Point were migrating across a variety of bedrock types and/or across a gradient of changing atmospheric contributions of strontium with different $^{87}Sr/^{86}Sr$ values, then intra-tooth or inter-tooth strontium isotope values should also reflect these changes.

2.4 Bioavailable Strontium Isotopes Across the GCFR

Bioavailable strontium has not been well documented across the GCFR, but a bioavailable strontium isoscape of the region is necessary in order to test the migration hypothesis using strontium isotopes of fossil tooth enamel. Measuring $^{87}Sr/^{86}Sr$ in plants has been demonstrated to be a reliable and consistently available method for determining

local bioavailable $^{87}Sr/^{86}Sr$ (Copeland et al., 2011; Durante et al., 2013; Evans et al., 2009; Maurer et al., 2012; Poszwa et al., 2009; Warham, 2011), and we employ this method to create an empirically based strontium isoscape. We have also created a geospatial model of our strontium isoscape in order to explore several issues. For example, can a geospatial model based on our empirical values be used to accurately interpolate bioavailable strontium values in areas not sampled directly by plants, such as the now-submerged Paleo-Agulhas Plain? Can it identify previously unknown factors that might control bioavailable $^{87}Sr/^{86}Sr$ or determine the best sampling strategy by which to approach future bioavailable $^{87}Sr/^{86}Sr$ studies that expand our current region?

Our approach to developing a strontium isoscape was as follows: 1) collect empirical data on modern bioavailable strontium by sampling plants across different geological substrata in the study area, 2) create a geospatial model to explore its predictive capabilities, 3) identify factors that are likely to govern the spatial structure of bioavailable $^{87}Sr/^{86}Sr$, such as geology and atmospheric sources, and 4) project this knowledge to estimate the bioavailable strontium across ancient landscapes including the exposed Paleo-Agulhas Plain.

The study area for the bioavailable $^{87}Sr/^{86}Sr$ isoscape is along the southern coast of the GCFR and aims to include the area that might have been utilized by the local and potentially migrating animals that were fossilized at the Pinnacle Point caves. The bioavailable $^{87}Sr/^{86}Sr$ sampling strategy was designed to sample multiple locations in each of the major geological groups, from the coast to the interior, and across the major physiographic units (following Marean et al. 2014). These physiographic units include the east-west trending Cape Fold Mountains, which can be divided into the southern

Outeniqua Mountains and the northern Swartberg Mountains, the intermontane basin between them known as the Little Karoo, the area north of the Swartberg Mountains known as the Great Karoo (we sampled only the southern edge of this vast area), the foothills south of the Outeniqua Mountains that grade into dissected plains near the coast, and a true coastal plain, the Paleo-Agulhas Plain, that is mostly currently underwater but is preserved as isolated small remnants between the Cape Agulhas and De Hoop Nature Reserves (Thwaites and Cowling, 1988).

3. METHODS

3.1 Fossil Localities – PP13B and PP30

PP13B is a sea cave formed in the Table Mountain Sandstone cliffs of Pinnacle Point that has preserved MSA archaeological deposits. It has geogenic deposits that date from MIS 11 at ~400 ka to ~160 ka (Jacobs, 2010; Marean et al., 2010). Archaeological deposits in the cave date from MIS 6 (~160 ka) to 90 ka in MIS 5 when the site was sealed by a dune, and that was not breached until sometime after ~40 ka. The majority of the teeth sampled here come from sediments dated to MIS 5d and MIS 5c and during this time the coast was up to 10 km distant (Fisher et al., 2010), though there is one specimen that comes from the MIS 6 deposits, and two from the MIS 3 deposits (Table 1). People were the primary accumulators of the PP13B fauna throughout its deposition (Thompson, 2010) and hunter-gatherers exploit a daily foraging radius that is rarely greater than 10-15 km (Kelly 1995; Marlowe, 2005).

PP30 is a paleontological site formed in the calcretes on the cliff top about one kilometer from the modern coastline, and the primary accumulator was the brown hyena

(*Parahyaena brunnea*). There are two optically stimulated luminescence (OSL) ages both at ~151 ka (Rector and Reed, 2010), and thus it samples a time when MIS 6 was in nearly maximum glacial conditions and the coast was far from where it is today, as much as ~95 km distant (Fisher et al., 2010). In contrast to the PP13B fossils that date to a variety of different time periods within the Pleistocene, all fossils from PP30 are likely to be similar in age. Brown hyenas provision their young with food, including ostrich eggs, which are abundant in the site, as well as primarily scavenged remains of large mammals. Brown hyenas are known to forage far, and in the Kalahari on average forage about 30 km at night (Mills 1990), suggesting that their foraging radius may somewhat exceed that of people. Because of their provisioning behavior, their dens tend to accumulate bones relatively quickly.

3.2 Sampling for Bioavailable $^{87}Sr/^{86}Sr$

At each of the 172 bioavailable $^{87}Sr/^{86}Sr$ sampling localities, we collected a handful of plant material from five different plants and combined those together before analysis (Table S2). In most cases, the plant growth forms present were grasses, forbs, or shrubs, so we collected a mixture of these. At four localities where there was a distinctive tree story and understory, we collected 5 plants from each and kept them as separate samples (Table S2). The plant material collected was mostly plant leaves, but also included some stems and seeds or fruits if present. All plant material was put into paper bags and allowed to dry inside the loosely packed bag.

Land snail shells were also collected at seven of the plant sampling localities. Snail shells typically contain high strontium concentrations and have been considered

possible proxies for bioavailable strontium (Blum et al., 2000), but in some previous studies discrepancies were shown to exist between $^{87}Sr/^{86}Sr$ of snails versus plants (Evans et al., 2009; Maurer et al., 2012). The results of our snail samples are presented in the Supplemental Information text. We chose not to use the snail results in the development of our bioavailable strontium isoscape because of the concerns mentioned above.

Sampling localities were chosen to represent the variety of bedrock types in areas as far away as possible from disturbances such as agriculture and development. The geologist (HC), who has substantial experience in the GCFR, was present during sampling and confirmed that the local bedrock at each locality matched that identified from the 1:250,000 or 1:50,000 geological map of the region. GPS readings were taken at each sampling locality (Table S2).

3.3 Fossil specimens

We sampled a total of 55 mammalian individuals: 32 individuals from PP30 and 23 individuals from PP13B representing a total of 12 taxa (Table 1 and Table 2) (Rector and Reed, 2010). The sampling strategy was designed to measure both potentially migratory and non-migratory species from the two sites, and to get serial samples for individuals through either intra-tooth sampling, sampling of successively forming teeth, or both. The dental faunal sample from PP13B is rather small, which restricted the number of individuals that we could sample. When possible, we chose to sample later forming teeth (M3) in order to ensure that the signal represents the post-weaning diet of the individual. In some cases the only available sample was M1 or M2 (or "M1/M2" when it was not possible to identify whether the tooth was M1 or M2). Several of the

374 fossil specimens preserved multiple teeth, in which case we obtained samples from up to
375 four teeth including the late-forming permanent premolar P4.
376 Information on the precise timing of tooth mineralization for the ungulates
377 sampled in this study was not available in the published literature to our knowledge, but
378 approximations can be made based on similar, well-studied species and reports of tooth
379 eruption times used for age determination (Table S3). In ungulates, molars typically
380 mineralize in a sequential manner in which enamel formation follows an uninterrupted
381 and slightly overlapping sequence from apex to neck in permanent first molars (M1),
382 second molars (M2), and third molars (M3). In modern cow (*Bos taurus*) and bison
383 (*Bison bison*), M1 mineralizes over approximately 6 months from the age of 3 months
384 before birth to 3 months old, M2 mineralizes over a year from one month old to 13
385 months old, and M3 mineralizes over a 15 month period from 9 to 24 months old (Brown
386 et al., 1960; Gadbury et al., 2000). In domestic sheep (*Ovis aries*), the M1 crown forms
387 from 2 months before birth to 6 months of age, M2 forms from 1 to 12 months of age,
388 and M3 starts to form at 10 months and is complete by 22 months (Zazzo et al., 2010).
389 Herbivores with very high-crowned molars have extended periods of tooth development,
390 for example, the M1, M2, and M3 of modern domestic horses (*Equus caballus*)
391 mineralize over periods of approximately 32 months, 30 months, and 34 months,
392 respectively (Hoppe et al., 2004). The relatively low-crowned molars of very small
393 steenbok (*Raphicerus campestris*) from South Africa were the subject of detailed intra-
394 tooth carbon and oxygen isotope analysis (Balasse et al., 2002). The observed sinusoidal
395 patterns indicate seasonal fluctuations and suggest that the steenbok M2 crown
396 mineralized over about six months, while the M3 crown mineralized over the following

six months. Published radiographs of known-age springbok (*Antidorcas marsupialis*) indicate that their molar mineralization times are very similar to that of cows and bison (Rautenbach, 1971).

Based on approximate tooth crown size and, in some cases, reported eruption patterns (see Table S3), the animals sampled in this study fall into roughly three groups in terms of permanent molar crown formation times. The first group has small molars (about 12 mm crown height) that each mineralize over about a 6 month period – these include the small steenbok (*R. campestris*) and grysbok (*Raphicerus melanotis*) (Balasse et al., 2002). The second group of species are larger and more hypsodont with crown heights for M2 and M3 around 20-30 mm. According to their eruption patterns (Table S3), these species have molar mineralization times similar to that of cows, bison, and sheep in which M1s form over about 6 months, while M2s and M3s take a year or slightly more. This second group includes hartebeest (*Alcelaphus*), springbok (*Antidorcas*), and reedbuck (*Redunca*). The third group consists of animals with very hypsodont molars with M2 and M3 crown heights on the order of 50-70 mm, similar to modern horses (Hoppe et al., 2004). In these individuals, the M1 likely takes from one to three years to form, while M2s and M3s form over about two to three years. These species include the wildebeest (*Connochaetes gnou*), eland (*Taurotragus oryx*), extinct giant buffalo (*Syncerus antiquus*), and zebra (*Equus* cf. *quagga*).

These approximations of tooth mineralization times can be used to estimate the number of seasons represented by intra-tooth or inter-tooth samples. All species analyzed in this study have sufficient intra- or inter-tooth samples to represent seasonal differences with the exception of the single *Panthera leo* sample on a P4.

3.4 Fossil Sampling Methods

In total, we analyzed 160 enamel and 5 dentine powder samples for strontium isotopes (Table S4). Samples of enamel powder (~4 mg) were obtained by gently abrading the side of premolars or molars using a handheld drill (UP-200 model, KUPA Inc.) equipped with a ¾ mm diameter spherical diamond drill bit (Figure S1). When possible, multiple parallel samples (up to six) were taken along the same side. The sampling line was on average 1.5-2.0 mm wide and its length was determined by the width of the tooth or lobe. The distance between the center points of intra-tooth samples was on average 5 mm, but varied from 3 to 9 mm with the exception of one *Connochaetes* specimen in which the two sub-samples that produced results were 23 mm apart. For some of the smaller teeth and broken teeth, the sampling "line" was up to 5 mm wide because it was not possible to obtain enough powder from a 2 mm line, or chips of broken tooth enamel were analyzed in lieu of powder. The specifics for each case are identified in Table S4.

In the results, intra- and inter-tooth samples are presented using the "cumulative distance from neck" measurement following Price et al. (2015). The cumulative distance from neck anchors the distance from neck measurements of all the teeth from one specimen to the neck of the latest forming tooth that was sampled at zero. For each species, the maximum observed crown height (from neck to occlusal surface) for each tooth type was calculated based on the specimens in hand, and this was used to transform, for example, distance from neck measurements from M1 and M2 to cumulative distance from neck measurements that are relative to the M3. The correction factors that are based

443 on observed crown heights are presented in Table S4. In order to visualize the
444 approximate relative time order for the samples in Figure 3, the results are presented on
445 the x-axis in reverse order (M1-M2-M3-P4).

446 From five of the teeth on which dentine was already exposed, we took one sample
447 of dentine powder. Comparison of $^{87}Sr/^{86}Sr$ in dentine versus enamel can be useful for
448 assessing the possibility of diagenetic alteration of enamel strontium (Copeland et al.,
449 2010). Unlike dentine, enamel is more resistant to diagenetic contamination because of its
450 essentially non-porous structure with relatively large crystals and a low organic
451 component (Budd et al., 2000; Chiaradia et al., 2003; Hoppe et al., 2003; Lee-Thorp and
452 Sponheimer, 2003) . The results of the dentine analysis are presented in the Supplemental
453 Text and generally support the integrity of the enamel strontium in the fossil specimens
454 from PP13B and PP30. Dentine results are also plotted alongside enamel results in Figure
455 3.

456

457 ***3.5 Statistical Analysis of the Fossil Isotope Data***

458 We tested for evidence of animal movements by examining strontium isotope
459 ratios of fossil ungulate teeth in light of the bioavailable $^{87}Sr/^{86}Sr$ isoscape. For some
460 analyses, previously identified fossil taxa (Rector and Reed, 2010) were grouped into
461 categories based on modern observations and, in the case of extinct taxa, based on prior
462 expectations in terms of their feeding behaviors and propensity to migrate. Animals were
463 classified as "grazers" (primarily grass eating) or "browsers/mixed feeders," and as
464 "potentially migratory" or "non-migratory" (Table 2). In some analyses animals were
465 grouped according to the site from which they derived (PP13B or PP30) because the sites

represent different but overlapping time periods, and had different primary collectors (humans versus hyenas). Strontium isotope values among various groupings of fossils by site, feeding behavior, taxon, and propensity to migrate are not normally distributed and some also have unequal variances. Therefore, when comparing these groups we used the non-parametric Wilcoxon test and Kruskal-Wallis test. Statistical tests were performed using JMP Pro 11.1.1 software.

3.6 Laboratory Methods

Plant sample material was cut into <1 cm pieces and subsamples from each of the five plants from each sampling locality were combined in a porcelain crucible with a lid at the Department of Archaeology, University of Cape Town. Plant samples were ashed in a muffle furnace ramped at 100°C/hour to 500°C and held at that temperature overnight.

Strontium isotope analysis was performed in the Department of Geological Sciences at the University of Cape Town. Twenty-five mg of ashed plant material per sample was digested in 2 ml of 4:1 mixture of 48% 2B HF: 65% 2B HNO_3 in a closed Teflon beaker placed overnight on a hotplate set at 140ºC. Following two stages of dry down and re-dissolving in 1 ml 65% 2B HNO_3, 2 ml 2M HNO_3 was added and allowed to settle overnight. 1.5 ml of liquid was pipetted out and centrifuged at 4000 rpm for 20 minutes, and the resulting clear supernate was collected for strontium separation chemistry. Similarly, up to 4 mg of each tooth enamel or dentine powder sample was dissolved in 2 ml 65% 2B HNO_3 in a closed Teflon beaker, and placed on a hotplate at 140°C for an hour. It was dried down and re-dissolved in 1.5 ml 2M HNO_3 for strontium

separation chemistry. Strontium separation chemistry for all samples followed the method of Pin et al. (1994).

The separated strontium fraction for each sample was dried down, dissolved in 2 ml 0.2% HNO_3 and diluted to 200 ppb Sr concentrations for isotope analysis using a Nu Instruments NuPlasma HR MC-ICP-MS. Analyses were referenced to bracketing analyses of NIST SRM987, using a $^{87}Sr/^{86}Sr$ reference value of 0.710255. All strontium isotope data are corrected for isobaric rubidium interference at 87 amu using the measured signal for ^{85}Rb and the natural $^{85}Rb/^{87}Rb$ ratio. Instrumental mass fractionation was corrected using the measured $^{86}Sr/^{88}Sr$ ratio and the exponential law, and a true $^{86}Sr/^{88}Sr$ value of 0.1194. Results for repeat analyses of an in-house carbonate standard processed and measured with the batches of unknown samples in this study ($^{87}Sr/^{86}Sr$ = 0.708920; 2 sigma = 0.000030; n = 7) are in agreement with long-term results for this in-house standard ($^{87}Sr/^{86}Sr$ = 0.708907; 2 sigma = 0.000023; n = 56).

3.7 Geospatial Modeling of the Strontium Isoscape

We used ESRI ArcGIS 10.3 to develop a predictive model of bioavailable $^{87}Sr/^{86}Sr$ across our study area using the observed $^{87}Sr/^{86}Sr$ measurements of the modern plant samples. Fifteen percent (15%) of the original sample of data points (n = 26) were extracted from the model development and used later to test the model predictions. The remaining points (n = 148) were imported into the ESRI Geospatial Analyst to develop our variographic model predicting $^{87}Sr/^{86}Sr$ distribution across the study area. We used the ordinary kriging method because we wanted to simultaneously map the predicted values and their standard errors across the landscape. We also did not assume that the

512 $^{87}Sr/^{86}Sr$ assumed a constant mean value across the study area. Results and further details
513 are presented in section 4.2.
514
515 **4. RESULTS**
516 ***4.1 Results of Modern Bioavailable $^{87}Sr/^{86}Sr$***
517 Strontium isotope ratios of modern plants from the 172 sampling sites across the
518 region ranged from 0.7092 – 0.7254 (Table S2). As seen in Figure 4, bioavailable
519 $^{87}Sr/^{86}Sr$ ratios from the Gamtoos/Malmesbury Group (0.7095 – 0.7157), Table Mountain
520 Group (0.7092 – 0.7169), General Neogene/Quaternary deposits (0.7104 – 0.7162), Cape
521 Granite Suite (0.7095 – 0.7177), Uitenhage Group (0.7101 – 0.7197), and Bokkeveld
522 Group (0.7093 – 0.7209) broadly overlap. Bioavailable $^{87}Sr/^{86}Sr$ from the Cango Caves
523 Group (0.7187 – 0.7254) and Witteberg Group (0.7164 – 0.7237) have the highest
524 average values, and come from the northernmost portions of the study area. Bredasdorp
525 Group samples (0.7092 – 0.7101) cluster tightly with the lowest average bioavailable
526 $^{87}Sr/^{86}Sr$ and are from the coast or near the coast (up to 22 km inland) on the modern
527 exposed Agulhas plain (Figure 2). The Bredasdorp Group consists of marine-derived
528 calcareous Neogene and Quaternary sediments such as beach deposits and dunes with
529 high fractions of shell, aeolianites, and calcarenites, so its bedrock $^{87}Sr/^{86}Sr$ is expected to
530 be close to the Quaternary marine value of 0.7092. Overall, the range of strontium
531 isotope ratios within calcareous rocks tends to be less than in non-calcareous rocks.
532 Although bioavailable strontium isotope ratios vary within most of the geological
533 groups, there is an overall pattern of increasing $^{87}Sr/^{86}Sr$ with increasing distance from
534 the coast. Distance to coast is a stronger predictor of bioavailable $^{87}Sr/^{86}Sr$ ($R^2 = 0.77$)

than latitude alone (R^2 = 0.68), while longitude shows almost no relationship (R^2 = 0.03) (Figure 5). Bioavailable $^{87}Sr/^{86}Sr$ from localities directly on the coast have the lowest values approaching that of modern seawater (0.7092) regardless of geology. For example, plants sampled from the modern exposures of the Agulhas Plain have $^{87}Sr/^{86}Sr$ ratios of 0.7092 – 0.7107 and are mainly from Bredasdorp Group sediments, but some were growing on Bokkeveld Group, Table Mountain Group, and Uitenhage Group geological substrates (Figure 2). Sampling localities on the dissected coastal plain have intermediate plant values of 0.7095 – 0.7172, and occur on Table Mountain Group, Bokkeveld Group, Uitenhage Group, Cape Granite Suite, and Gamtoos/Malmesbury Group geological substrates. Sampling sites from the intermontane basin (Little Karoo) have plant $^{87}Sr/^{86}Sr$ ranging from 0.7124 – 0.7202, and occur on Table Mountain Group, Bokkeveld Group, Uitenhage Group, General Neogene/Quaternary deposits, Cango Caves Group, and Witteberg Group geological substrates. Sampling sites from northernmost portions of our study area, north of the Swartberg Mountains in the Great Karoo, have plant $^{87}Sr/^{86}Sr$ ranging from 0.7168 - 0.7237, and occur on Table Mountain Group, Bokkeveld Group, and Witteberg Group geological substrates. Samples within the Cango Caves Group and the Witteberg group, which are at least 65 and 78 km away from the coast, respectively, show a weak or inverse relationship of $^{87}Sr/^{86}Sr$ with distance to coast (Figure S2).

4.2 Results for Geospatial Modeling of the Strontium Isoscape

The geospatial distribution of bioavailable $^{87}Sr/^{86}Sr$ is skewed heavily towards values <0.7110. Samples having values <0.7110 were located entirely within 20 km of the current coastline and likely indicate a zone of increased marine influence on

bioavailable $^{87}Sr/^{86}Sr$. Otherwise, intragroup analysis of the localities grouped by <20 km and >20 km from the modern coastline showed more normally distributed $^{87}Sr/^{86}Sr$ values.

We fitted different semivariogram models to the data and observed the prediction errors. Testing for various semivariograms and their parameters revealed that the $^{87}Sr/^{86}Sr$ values were anisotropic on a bearing of ~78°, which is roughly in line with the orientation of the Cape Fold mountains, the generally east-west trending geological strata, and the modern coastline. A spherical semivariogram provided the smallest mean (-0.0000) and standardized mean (-0.0015), indicating unbiased prediction errors. The root mean squared prediction errors were also low (0.0017) and only differed from the average standard error (0.0013) by a value of 0.0004, which indicates a robust assessment of variability in the model predictions. The model parameters and results are provided in Table S5 and S6. The final bioavailable $^{87}Sr/^{86}Sr$ geospatial model is shown in Figure 6.

When the variability in the standard error from the model predictions is mapped across the study area it is fairly evenly distributed. That variability is likely to be underestimated subtly, however, as indicated by the slightly elevated standardized root mean square value of 1.3102. Moreover, we observed that there was a rapid increase in the standard error of the model predictions approximately 25 km away from the sample locations. In normally distributed datasets, accurate predictions should occur within 2x the average standard error 95% of the time. The ~25 km buffer coincided with the 0.0026 isohyet, which is 2x our average standard error, and thus it can be used to demarcate reliable (<0.0026) and unreliable (>0.0026) model predictions. We used this 25 km buffer to exclude model predictions that we consider to be unreliable.

After the model was created it was validated using the subset of points removed from the original dataset. The absolute difference between the subset $^{87}Sr/^{86}Sr$ values and model predictions is small – having a mean of 0.0012 – and also consistent with a standard deviation of just 0.0012.

Thereafter, we projected 100,000 points randomly across the study area and extrapolated the predicted model results at each of these locations. We also derived the lithological group at each point by spatially joining these points to the 1:250,000 geological classifications provided by the South African Council for Geoscience. All points from areas that fell outside of our 25 km buffer were subsequently removed, which resulted in a total data set of 68,338 points for comparisons.

We grouped these 68,338 points by geology and compared the mean predicted values with the mean observed values (empirically measured plants) from each geological type. These data are included in Table S5 alongside the predicted descriptive statistics from the geospatial model. The absolute differences between the observed and predicted mean $^{87}Sr/^{86}Sr$ values for each geological group ranged up to 0.0053 (Gamtoos/Malmesbury Group), but in general were low ($\overline{x} = 0.0022, sD = 0.0018, p = 0.001$). Linear regression between the observed and predicted bioavailable $^{87}Sr/^{86}Sr$ values resulted in $R^2 = 0.52$ ($p < 0.05$). When the Gamtoos/Malmesbury Group and Cango Cave Group points (related geologically) were removed from the regression then the $R^2 = 0.73$ ($p < 0.05$).

4.3 Results for $^{87}Sr/^{86}Sr$ of Fossil Teeth

The strontium isotope ratios of tooth enamel from the 55 fossil individuals from

PP13B and PP30 fell within a range that is considerably smaller than that of the modern plants (Figure 4). Fifty-three individuals had $^{87}Sr/^{86}Sr$ from 0.7092 to ~0.7101, while one wildebeest and one eland had higher ratios of ~0.7110. In general, the strontium isotope ratios were far more variable between individuals than within serial samples from each individual (Figure 3). Among all individuals with two or more intra- or inter-tooth samples, the average difference between maximum and minimum serial $^{87}Sr/^{86}Sr$ ratios was 0.00006.

Strontium isotope ratios of animals from PP13B considered as a group (0.7098 ± 0.0005, n=23) were significantly higher than those from PP30 (0.7094 ± 0.0001, n=32; p=0.003). Potentially migratory animals (Table 1) at PP13B (0.7099 ± 0.0005) had on average higher $^{87}Sr/^{86}Sr$ than non-migratory animals from the same site (0.7093 ± 0.0001, p=0.002), but this pattern was not found at PP30 (potentially migratory animals 0.7095 ± 0.0001; non-migatory animals 0.7095 ± 0.0001). There was no difference in $^{87}Sr/^{86}Sr$ between species typically considered grazers versus those typically considered browsers and/or mixed feeders at either PP13B (grazers 0.7099 ± 0.0004; browsers 0.7097 ± 0.0006; p=0.06) or PP30 (grazers 0.7095 ± 0.0001; browsers 0.7094 ± 0.0001; p=0.16).

There are differences between $^{87}Sr/^{86}Sr$ by genera when specimens from both sites are combined (Kruskal-Wallis Test; genera with only one individual excluded; p=0.0046) (Figure 7). A Wilcoxin test on each pair (one-tailed) indicates that *Raphicerus* has lower $^{87}Sr/^{86}Sr$ than *Alcelaphus* (p=0.008), *Antidorcas* (p=0.001), *Connochaetes* (p=0.004), and *Redunca* (p=0.023). Among genera represented by more than one individual, *Connochaetes* and *Antidorcas* have the highest variances between individuals and *Raphicerus* has the lowest variance between individuals.

4.3.1 Results by Taxon

We sampled nine *Alcelaphus buselaphus* (hartebeest) individuals, six from PP30 and three from PP13B (Figure 3 and Figure 7). The hartebeest is a plains antelope that is often migratory, though less so than wildebeest (Estes 1991). The $^{87}Sr/^{86}Sr$ values are moderately variable between individuals, but inter- and intra-tooth variation is always less than 0.0001 in samples that represent 3 -12 months of tooth formation.

We sampled eleven individuals of the extant springbok species (*Antidorcas marsupialis*), five from PP13B and six from PP30, and five springbok of undetermined species (*Antidorcas* sp. indet.), all from PP13B. The extant springbok is a plains antelope that is typical of treeless landscapes, ranges across a wide variety of habitats, and has been known to migrate in vast herds (Skead, 2011). The sampled specimens have a relatively broad range of values, and those from PP13B are higher than those from PP30 ($p=0.002$) (Figure 7). Inter- and intra-tooth variation that represents more than six months of time (15 mm across the M3) on at least five individuals does not exceed 0.00009.

We sampled eight *Connochates gnou* (black wildebeest), three from PP13B and five from PP30. The black wildebeest is a true plains antelope and is typically migratory (Estes 1991). Specimen 41399 from PP13B has the greatest amount of intra-tooth variation (0.00046) seen within any single individual of the project, and has anomalously high values (mean = 0.71116). Its intra-tooth samples span 18 mm of the M1/M2 (one half to one third of the total crown height), which represents about 3-9 months of mineralization time (Table S3). For four other wildebeest specimens, intra-tooth samples spanning >18 mm on the M3 represent approximately 6-12 months of mineralization

649 time, but the maximum intra-tooth variation for these is only 0.00003. Wildebeest have
650 the highest variance between individuals of all genera.

651 *Raphicerus* (steenbok and grysbok) are small, sedentary antelopes with restricted
652 local home ranges (Skinner and Smithers, 1990). The 11 individuals that we sampled
653 have consistently low $^{87}Sr/^{86}Sr$ values (0.70925 – 0.70950) below the mean $^{87}Sr/^{86}Sr$ for
654 individuals of all taxa (0.70962; n=55). Steenbok and grysbok have the lowest variance
655 between individuals of all genera (Figure 7).

656 We sampled five *Redunca arundinum* (southern reedbuck) and two *Redunca*
657 *fulvorufula* (mountain reedbuck), all from PP30. Both are grazers, the former specializing
658 on wet edaphic grasslands and the latter on grassy slopes (Estes 1991). Although
659 reedbuck are also non-migratory, their mean $^{87}Sr/^{86}Sr$ values are higher ($p=0.023$) than
660 those of *Raphicerus*.

661 We sampled the only available molar from *Equus* cf. *quagga* (zebra), which was
662 an M3. Three intra-tooth samples spanning 11 mm, or about 3-6 months of mineralization
663 time, show a $^{87}Sr/^{86}Sr$ value of 0.70951 with an intra-tooth range of 0.00003. The zebra is
664 a plains animal that is sometimes migratory.

665 We sampled one extinct giant buffalo (*Syncerus antiquus*) mandible. The extinct
666 giant buffalo is thought to have been a plains grazer due to its hyper-hypsodont tooth row
667 (Klein, 1994). We took two intra-tooth specimens each from the M1, M2, and M3, which
668 show relatively low variation (0.00017) and a mean $^{87}Sr/^{86}Sr$ value of 0.70963. The time
669 "missing" between the samples on each tooth could be up to a year or more.

670 We sampled a single *Taurotragus oryx* (eland) M1/M2 with three intra-tooth
671 samples that represent about 3-6 months of mineralization time. Intra-tooth variation is

0.00013 and the $^{87}Sr/^{86}Sr$ value is extremely high, matched only by one wildebeest specimen.

We sampled a single *Panthera leo* (lion) from PP30 on its P4. Its $^{87}Sr/^{86}Sr$ value (0.70958) is extremely close to the mean $^{87}Sr/^{86}Sr$ for individuals of all taxa (0.70962; n=55).

5. DISCUSSION

5.1 Bioavailable strontium isoscape

The range of bioavailable strontium isotope ratios documented in plants across the south coast portion of the modern GCFR is 0.7092 - 0.7254 (Figure 4 and Figure 6). This is consistent with expectations, given that the end members of this system are strontium contributed from modern seawater (0.7092), and bedrock-derived strontium from either soil or dust. The bedrock-derived strontium from Bredasdorp limestone and other marine sediments along the modern coastline, and across much of the now-submerged Paleo-Agulhas Plain, should have $^{87}Sr/^{86}Sr$ ratios around 0.7092, since they derive predominantly from marine organisms. However, strontium from the Precambrian and Paleozoic bedrock that forms most of the Cape Fold Mountains and surrounding areas should have much higher $^{87}Sr/^{86}Sr$ ratios (Table S1). Published measurements of Malmesbury shale whole rock $^{87}Sr/^{86}Sr$ range from 0.721 – 0.787, consistent with expectations for a rock that is ancient and has relatively high rubidium to strontium ratios (Allsopp and Kolbe, 1965; Backeberg et al., 2011). Similarly, Cape Granite Suite whole rock $^{87}Sr/^{86}Sr$ ranged from 0.77 – 1.16 (Allsopp and Kolbe, 1965), and bedrock $^{87}Sr/^{86}Sr$ from the Table Mountain Group measured 0.747 (Midgley et al., 2012). Although the

strontium that becomes part of the bioavailable nutrients in soil as a result of bedrock decomposition may not have the same $^{87}Sr/^{86}Sr$ ratio as the parent whole rock values (Sillen et al., 1998), bedrock or dust-derived strontium from the Cape Fold Mountains and surrounding areas should nevertheless be substantially higher than modern marine values of 0.7092.

The strong correlation between bioavailable $^{87}Sr/^{86}Sr$ and distance to coast implies a heavy influence of marine-derived strontium (0.7092) to the bioavailable pool on the south coast portion of the modern GCFR (Figure 5, Figure S2). Marine-derived strontium has been shown to contribute substantially to bioavailable strontium in coastal regions around the world (Chadwick et al., 2009; Evans et al., 2010; Whipkey et al., 2000). Marine-derived strontium can be added to the onshore biosphere either directly as sea spray at or very near the coast, or more indirectly further inland in the form of fog and precipitation that derives from marine sources (Montgomery, 2010). Seawater (~8-9 ppm Sr) and sea salt (~22 ppm Sr) have considerably higher concentrations of strontium than most freshwaters (many are < 1 ppm Sr; Chesson et al., 2012; Culkin and Cox, 1966; Fenner and Wright, 2014; Horne, 1969; Montgomery et al., 2006; Odum, 1957; Voerkelius et al., 2010).

Most large intercontinental dust plumes are in the equatorial region or northern hemisphere, where they contribute strontium to biospheres in Hawaii, the Caribbean, and the eastern Mediterranean, among other places (Bataille et al., 2012; Chadwick et al., 2009; Hartman and Richards, 2014). There is less dust in the southern hemisphere overall (Bryant et al., 2007; Vickery et al., 2013). While dust may contribute some strontium to the GCFR system (Soderberg and Compton, 2007), much of that dust is likely to be

derived from local bedrock sources, thereby also containing local bedrock-derived $^{87}Sr/^{86}Sr$. Some dust may also come from the semi-arid Great Karoo north of the GCFR, which also has relatively high $^{87}Sr/^{86}Sr$ (de Villiers et al., 2000; Midgley et al., 2012).

Bioavailable $^{87}Sr/^{86}Sr$ along the south coast of the GCFR could change over time if the relative contribution of strontium from marine versus bedrock or dust changed. Since distance to coast from the Pinnacle Point caves has varied from 0 to 100 km throughout the late Pleistocene (Fisher et al., 2010), this is a possibility worthy of consideration. We can estimate the magnitude of change in bioavailable $^{87}Sr/^{86}Sr$ with changes in distance to coast using the $^{87}Sr/^{86}Sr$ measured in time sequence in speleothems from caves at Pinnacle Point as reported in Fisher et al. (2010). Speleothems are formed from seepage water within the caves, and the strontium within that seepage water likely derives from a combination of sources such as soil, bedrock, dust, sea spray, fog, and precipitation. As such, the $^{87}Sr/^{86}Sr$ ratios in speleothems are likely a good reflection of bioavailable $^{87}Sr/^{86}Sr$.

Fisher et al. (2010) found that $^{87}Sr/^{86}Sr$ in speleothems from Pinnacle Point caves dating from ~325 ka to the present vary through time as a function of distance from coast, as predicted by a model in which atmospheric marine-derived strontium contributes substantially to speleothem (and bioavailable) $^{87}Sr/^{86}Sr$. When the coast is very near, $^{87}Sr/^{86}Sr$ ratios in the speleothems tend to approach ~0.7092, the value of modern seawater, while greater distances to the coast (up to 100 km) correspond to higher values with a maximum of 0.70965 (Fisher et al., 2010), due presumably to a greater relative contribution of bedrock- or dust-derived strontium. However, this magnitude of change (~0.0005) is small relative to the variability of bioavailable strontium isotope ratios

741 across the entire region (0.7092 – 0.7254). It is less than the difference between some
742 modern plants growing on the Bredasdorp Group calcareous sediments (0.7092 –
743 0.7011). It is comparable to the maximum intra-tooth variability observed in one fossil
744 wildebeest from PP13B (0.00046). Thus, the low magnitude of change in speleothem
745 $^{87}Sr/^{86}Sr$ over the past 325 ka despite movement of the coast by 100 km indicates that
746 modern bioavailable $^{87}Sr/^{86}Sr$ in the area around and north of the current coastline is a
747 robust representation of bioavailable strontium distribution in the past. Although sea level
748 changes may have resulted in shifts in bioavailable $^{87}Sr/^{86}Sr$ at the coast of ~0.0005 at
749 and near the coast, this shift is insignificant compared to differences between bioavailable
750 $^{87}Sr/^{86}Sr$ near the coast versus near the Outeniqua Mountains, for example.
751 In order to reconstruct bioavailable strontium isotope values across the now-
752 submerged Paleo-Agulhas Plain, we draw upon evidence of the offshore geology, what
753 we have learned about how marine- and bedrock-derived strontium interact on the current
754 land surface, and predictions of the geospatial model.
755
756 ***5.2 Paleo-Agulhas Plain bioavailable strontium isoscape***
757 Although the present-day submerged Agulhas Bank is a highly eroded (Martin
758 and Flemming, 1986), oceanic current-dominated continental shelf (Johnson and
759 Baldwin, 1986), preserved Quaternary deposits include aeolianite, beach deposits, infilled
760 river channels and buried back-barrier sediments (Cawthra et al. 2014). Using seismic
761 and surficial geological data, Cawthra (2014; Cawthra et al., 2015) showed that during
762 the sea-level lowstand of MIS 6, shallowly incised rivers with broad adjacent floodplains
763 dominated the Paleo-Agulhas Plain, particularly in the vicinity of Mossel Bay (5 km east

764 of Pinnacle Point). A high abundance of carbonate in the system suggests active dune
765 sedimentation at this time, with likely exposure of the Neogene limestone deposits. The
766 successive glacial periods of MIS 4 and MIS 2 are interpreted to be associated with a
767 larger sediment supply of unconsolidated Bredasdorp Group sediments. Broad paleo-
768 coastal zones of dunefields likely swept the shelf at these times, burying the older
769 geological lithologies (Cawthra, 2014).

770 The hard-rock geological composition of the shelf beneath the modern marine
771 sediment wedge is characterized by a coast-parallel trending outcrop of Uitenhage Group
772 (Cretaceous) deposits directly adjacent to the modern coastline, immediately south and
773 east of Pinnacle Point with an additional component along the modern coast further to the
774 west (Figure 2). Modern on-shore Uitenhage Group exposures along the South Coast
775 have bioavailable $^{87}Sr/^{86}Sr$ from 0.7101 – 0.7197. The three Uitenhage sites that are less
776 than 4 km from the modern coast, and presumably have the greatest influence of marine-
777 derived strontium, have the lowest bioavailable $^{87}Sr/^{86}Sr$ ratios of 0.7101. The modern
778 Uitenhage range may be our best estimation of the bioavailable $^{87}Sr/^{86}Sr$ range of
779 Uitenhage exposures on the Paleo-Agulhas Plain when this bedrock was exposed at the
780 surface. At times, marine sands in the form of dunes, aeolianites, and other calcareous
781 sediments may have buried the offshore Uitenhage Group bedrock (Cawthra, 2014) and
782 contributed strontium to the biosphere with $^{87}Sr/^{86}Sr$ close to 0.7092. However, when
783 Quaternary sediments were stripped off the Cretaceous shales, the soils derived from
784 these rocks would have been fertile and would have likely supported Renosterveld with a
785 varying but generally high component of C4 grasses (Cowling, 1983; Cowling and Potts,
786 2015), depending on the amount of warm season rainfall. The modern, near-shore

787 Uitenhage sampling localities provide an estimate for bioavailable $^{87}Sr/^{86}Sr$ (0.7101) for
788 exposed Cretaceous shales.
789 South of the offshore Uitenhage Group deposits are belts of the Cape St. Blaize-
790 and Cape St. Francis Group sediments, that do not have equivalent exposures on the
791 contemporary coast (Figure 2). Both are predominantly Palaeogene and Neogene
792 limestones and calcareous clays (Dingle et al., 1983) and therefore are likely to have
793 whole rock $^{87}Sr/^{86}Sr$ ratios of approximately 0.7092 or slightly higher, with bioavailable
794 $^{87}Sr/^{86}Sr$ similar to the Bredasdorp Group (0.7092 – 0.7101). The Cape St. Blaize- and
795 Cape St. Francis Groups offshore were also likely covered in dune sands that would
796 further contribute toward a bioavailable $^{87}Sr/^{86}Sr$ ratio close to 0.7092.
797 Approximately 100 km southwest of Pinnacle Point on the Paleo-Agulhas Plain,
798 bedrock zones that may have been exposed at lower sea levels include Uitenhage Group
799 deposits, the Alphard Igneous Complex, Bokkeveld Group shales, and Table Mountain
800 Group sandstones (Figure 2). Based on direct analogy with their modern onshore
801 counterparts, the Uitenhage-, Bokkeveld-, and Table Mountain Group areas could have
802 had bioavailable $^{87}Sr/^{86}Sr$ ratios ranging from 0.7092 – 0.7209. However, it is likely that
803 they were covered either totally or partially in marine sands and influenced by direct sea
804 spray or marine-derived precipitation, all of which would tend to bring bioavailable
805 $^{87}Sr/^{86}Sr$ lower, closer to 0.7092. The Alphard Igneous Complex is composed of Tertiary
806 volcanic tuff, trachyte, and basalt (Dingle et al., 1983). As expected for young volcanics,
807 its whole rock strontium ratios are extremely low, around 0.7029 (Janney et al., 2002).
808 In sum, it is likely that most of the Paleo-Agulhas plain had bioavailable $^{87}Sr/^{86}Sr$
809 similar to, or even at the low end of, the modern Bredasdorp Group range of 0.7092 –

0.7101. The Palaeogene and Neogene-aged Cape St. Blaize- and Cape St. Francis Groups were likely to have whole rock values close to 0.7092. The Precambrian and Paleozoic bedrock geologies on the Paleo-Agulhas plain (e.g., Bokkeveld and Table Mountain Groups) likely have whole rock $^{87}Sr/^{86}Sr$ ratios that are much higher. However, seismic and surficial geophysical evidence on the South Coast (Cawthra et al., 2014; 2015) suggests that on the inner- and mid-shelf they were mostly covered with marine sands, aeolianites, or other calcareous sediments during times of lowered sea level. This sediment cover, along with marine-derived sea-spray, fog, and precipitation, likely swamped the bioavailable strontium isotope ratio, as is the case in current outcrops of these rocks near the coast. It is unlikely that anywhere on the Paleo-Agulhas Plain bioavailable $^{87}Sr/^{86}Sr$ ratios were higher than the range of the fossil animals with the possible exception of the older bedrock areas >100 km southwest of Pinnacle Point.

5.3 Implications for fossil animal movements

Comparison of $^{87}Sr/^{86}Sr$ values of the fossil animals analyzed from PP30 and PP13B to the isoscape model suggests that the animals spent little or no time substantially north of the current coastline. The predominant range of strontium isotope values in the fossils (0.7092 – 0.7101) is consistent with bioavailable strontium isotope ratios on modern exposures of Bredasdorp Group and the coastal plain, including some sites on Table Mountain Group, Bokkeveld Group, Cape Granite Suite, and Gamtoos/Malmesbury Groups near the coast (see similar results in Radloff et al., 2010). The fossil values are also consistent with most areas of the Paleo-Agulhas Plain when it was exposed, as suggested by our strontium isoscape model. Since there is no reason to

infer that bioavailable $^{87}Sr/^{86}Sr$ of the interior (the dissected plain, Cape Fold Mountains, Little Karoo, and Great Karoo) ever received a greater contribution of marine-derived strontium than at present, interior bioavailable strontium isotope ratios have probably been the same as today or higher since MIS 6. The two animal individuals from PP13B with the highest $^{87}Sr/^{86}Sr$ ratios of ~0.711 (a wildebeest and an eland) could have spent time on the dissected plain, but probably spent very little or no time in the area north of the Outeniqua Mountains, which has bioavailable $^{87}Sr/^{86}Sr$ ranging from 0.712 – 0.724, at least while their teeth were mineralizing. Taken together, the pattern suggests that grazing opportunities on the Paleo-Agulhas Plain were considerably more attractive than areas to the north of the modern coastline

The low intra-tooth strontium isotope variability in nearly all individuals (Figure 3) suggests either that they were not moving much during the time of tooth formation, or that if they were moving, it was along a region of relatively constant bioavailable strontium isotope ratios. Since bioavailable $^{87}Sr/^{86}Sr$ varies with a strong gradient from south to north (at least north of the modern coastline), but not from east to west, the unchanging intra-tooth values of nearly all fossil individuals could be consistent with east-west movements. However, they are inconsistent with large north-south movements in the region north of the modern coastline. Several of the species analyzed are known to migrate long distances (wildebeest, springbok, zebra), so unless their behaviors were substantially different in the Pleistocene, east-west movements are still a strong possibility. Additional analyses using carbon isotopes might help to resolve this issue since the proportion of C_4 grasses increases from west to east (Cowling, 1983; Vogel et al., 1978).

856 Animals from PP13B (0.7098 ± 0.0005) have higher $^{87}Sr/^{86}Sr$ ratios than animals
857 from PP30 (0.7094 ± 0.0001). This could be due to differences in the areas of the
858 landscape used by animals and/or differences in bone accumulators at these two sites.
859 PP30 dates to 151 ka when sea level was lower and the coast is modeled to be 95 km
860 away (Fisher et al., 2010). PP13B fauna come from several different time periods, but the
861 biggest sub-sample (n=11) is from the "Roof Spall-Upper" stratigraphic aggregate that
862 dates to 91-98 ka when the coast is modeled to be less than10 km away (Fisher et al.,
863 2010). Within the Roof Spall-Upper stratigraphic aggregate, shellfish assemblages
864 collected by people include substantial portions of both sandy beach and rocky intertidal
865 zone species, suggesting that the coast was within the daily foraging radius of hunter-
866 gatherers, which rarely exceeds 10-15 km. If local bioavailable $^{87}Sr/^{86}Sr$ at Pinnacle Point
867 itself changed slightly with sea levels along the magnitude suggested by changes in the
868 PP speleothems (~0.0005) (Fisher et al., 2010), then we would expect slightly higher
869 values during PP30 times when the coast was further away.
870 Since the PP30 animals actually have lower $^{87}Sr/^{86}Sr$ than the PP13B animals, the
871 PP30 animals were probably spending most of their time on the widely exposed Paleo-
872 Agulhas Plain with its relatively low strontium isotope ratios. In contrast, some PP13B
873 animals may have been forced to spend more time in the immediate vicinity and north of
874 the modern coastline because a smaller extent of the Paleo-Agulhas Plain would have
875 been exposed during their lifetimes. This would mean that the animals sampled at PP13B
876 foraged further onto the dissected plain where there are a greater variety of rock types,
877 fewer calcareous rocks, and higher bioavailable strontium isotope ratios. The fact that the
878 wildebeest and eland with the highest $^{87}Sr/^{86}Sr$ values are both from PP13B is consistent

879 with this interpretation.

880 During the accumulation of PP30, the coastal plain was so large that it may have
881 supported a large mammal ecosystem. In the modern and historic GCFR, Renosterveld is
882 regarded as the biome best able to support a large biomass of grazers (Boshoff et al.,
883 2001; Boshoff and Kerley, 2001). Renosterveld occurs across the dissected plain north of
884 the modern coastline on the relatively high $^{87}Sr/^{86}Sr$ Bokkeveld shales. It may have been
885 present on portions of the exposed Paleo-Agulhas Plain near the modern coastline if
886 Quaternary sediments were stripped from the Cretaceous shales, contributing to localized
887 areas of slightly higher bioavailable $^{87}Sr/^{86}Sr$. That animals during PP30 times appear to
888 have been using the Paleo-Agulhas Plain and not the dissected plain, even though the site
889 of PP30 itself is along the border of these two landforms, suggests that the Paleo-Agulhas
890 plain provided the preferred habitats.

891 Another possible explanation for the slightly higher $^{87}Sr/^{86}Sr$ at PP13B could be
892 related to the differing accumulators, which were humans at PP13B and brown hyenas at
893 PP30. It is possible that humans were hunting further afield and in a wider variety of
894 habitats such as those found in the dissected plain, while the hyenas at PP30 focused only
895 on the Paleo-Agulhas Plain. Even if this were the case, however, the overall trend of low
896 $^{87}Sr/^{86}Sr$ values among the animals relative to bioavailable $^{87}Sr/^{86}Sr$ across the broader
897 region implies that in general they preferred Paleo-Agulhas Plain or modern coastline
898 areas over areas further to the north.

899 Among comparisons between the various animal genera, the only statistically
900 significant difference is that small *Raphicerus* antelopes have lower strontium
901 isotope values that are tightly clustered, regardless of whether they are from PP30

or PP13B. Since *Raphicerus* are known to have small home ranges and are territorial, these animals may be more representative of the "local" bioavailable strontium isotope values.

5.4 Alternative hypotheses for animal movement

Ungulate movements on the Pleistocene south coast of the GCFR could have operated in a number of ways. Our study was designed to test the Paleo-Agulhas Plain migration ecosystem hypothesis, which posits an eastern-summer to western-winter movement pattern, and an alternative hypothesis that ungulates moved between the interior and the coast. The Outeniqua Mountains separating the inter-montane basin (the Little Karoo) from the coastal plains are not particularly high (no more than 1400 meters above sea level) and do have passes, so such a migration pattern is possible. Some historical accounts suggest that north to south animal movements occurred among elephants (Skead 2011). The strontium isotope analysis of fossil teeth, as informed by the bioavailable strontium isoscape, has the potential to falsify the east-west migration hypothesis and test the north-south hypothesis. If the serial measurements showed large changes in $^{87}Sr/^{86}Sr$ from high values to low values, this would be supportive of a north-south movement and unsupportive of an east-west movement. The results of fossil teeth $^{87}Sr/^{86}Sr$ cannot falsify the east-west migration hypothesis, but do falsify a hypothesis of north-south movement. The evidence that ungulates did not move north of the Outeniqua Mountains suggests that the Pleistocene grazing ungulate communities of the intermontane basin (the Little Karoo) documented at sites such as Boomplaas (Faith,

924 2013), and those on the south coast sampled by PP30 and PP13B (Rector and Reed,
925 2010) were separate populations.
926 An alternative hypothesis is that ungulates in this region spent a significant
927 amount of time on the foothills and dissected coastal plain south of the Outeniqua
928 Mountains and north of the now-submerged Paleo-Agulhas Plain, and in general moved
929 about the landscape utilizing patchy high quality graze, such as that in Renosterveld, in
930 patches of nutrient-rich Bokkeveld Group shale sediments in the dissected plain (Radloff
931 et al., 2010). In this scenario, we would expect strontium isotope ratios that are higher
932 than those of bioavailable $^{87}Sr/^{86}Sr$ from the Bredasdorp Group and other areas
933 immediately along the modern coast. The Bokkeveld Group shales appear to produce
934 relatively high $^{87}Sr/^{86}Sr$ ratios that are overwhelmed by the abundance of marine-derived
935 strontium (lower$^{87}Sr/^{86}Sr$) in the biosphere near the coast (Figure S2). Bokkeveld shales
936 more than 30 kilometers north of the modern coast have bioavailable $^{87}Sr/^{86}Sr$ greater
937 than 0.712, while those from the interior can be higher than 0.720 (Table S2). The
938 $^{87}Sr/^{86}Sr$ ratios in the fossils (0.709 – 0.711) are lower than would be expected if animals
939 spent much time on Bokkeveld/Renosterveld, unless it was in patches near the coast or on
940 exposed Cretaceous shales along the northern Paleo-Agulhas Plain. Comparison to the Sr
941 isoscape model shows that the region of similar bioavailable Sr values to the fossils
942 occurs predominantly on the exposed Paleo-Agulhas Plain and within the region ~15 km
943 inland on the coastal plain. Thus, the strontium pattern measured in the fossils is most
944 consistent with the ungulates spending the majority of their lives on marine-derived or
945 seawater influenced sediments on or within about 15 km of the Paleo-Agulhas Plain.

946 Flowing south from the intermontane basin (Little Karoo) and dissected plain are
947 several drainages that cut through Bokkeveld Group shales on their way to the south
948 coast. During times of lower sea level, as they drained onto the flat Paleo-Agulhas Plain,
949 they may have spread the nutrient-rich alluvium in north-south running strips (Marean et
950 al., 2014). These would be high quality grazing areas favored by ungulates. Bokkeveld-
951 /nutrient-rich soils have higher $^{87}Sr/^{86}Sr$ ratios than the Bredasdorp or other marine-
952 derived sediments but can be swamped by marine-derived strontium. The relatively low
953 $^{87}Sr/^{86}Sr$ ratios of the fossil teeth suggest that these alluvium locations were not present,
954 or that they were not significantly grazed by the sampled ungulates. Alternatively, the
955 Bokkeveld-/nutrient-rich soils might have been present, but contributed little strontium to
956 the biosphere compared to marine-derived sea-spray, precipitation, and sediments on the
957 relatively flat Paleo-Agulhas Plain. Offshore geophysical studies favor the explanation
958 whereby such floodplain deposits were rapidly overlain, at least partially, by marine
959 sediments such as sand dunes (Cawthra 2014). This would add marine-derived strontium
960 resulting in bioavailable $^{87}Sr/^{86}Sr$ ratios closer to 0.7092.
961
962 **6. CONCLUSIONS**
963 We created a bioavailable $^{87}Sr/^{86}Sr$ isoscape for the south coast of the GCFR
964 region by analyzing plants from 171 sampling sites and developing a geospatial model.
965 This provided a robust isoscape for interpreting the movement patterns of fossil ungulates
966 dating to the Middle and Late Pleistocene from Pinnacle Point. Results indicate that
967 ungulates did not spend significant amounts of time foraging on mountain, foothill, or
968 dissected plain localities more than about 15 km north of the modern coastline. The

results clearly exclude a north-south, interior-coastal movement or migration pattern. The strontium isotope evidence shows that these fossil ungulates foraged primarily on the now-submerged Paleo-Agulhas Plain habitats rather than those north of the modern coast line. This suggests that the open-habitat fauna that dominate the Pleistocene assemblages on the south coast derive from a population of animals largely restricted to the now-submerged Paleo-Agulhas Plain. Given this specialized use of this plain, this animal community would have suffered catastrophic habitat loss when sea levels rose during the Holocene and MIS 5e. Since bioavailable strontium varies from north to south but not from east to west, other isotope systems such as carbon and oxygen may be better suited for testing east-west movements based on fossil tooth enamel.

Acknowledgements

We would like to thank Jan Vlok for botanical expertise and help with sample collections, Kerryn Gray, Fayrooza Rawoort, and Hope Williams for help with laboratory analyses, John Lanham, Ian Newton, and Judith Sealy for support at the UCT Department of Archaeology stable isotope laboratory, and Paul Sandberg and Matt Sponheimer for helpful discussions. We would like to thank the anonymous reviewers, whose comments helped us to improve the manuscript. This research was funded by the National Science Foundation (# BCS-9912465, BCS-0130713, BCS-0524087, and BCS-1138073), the Hyde Family Foundations, the John Templeton Foundation, and the Institute of Human Origins (IHO) at Arizona State University. The opinions expressed in this publication are those of the author(s) and do not necessarily reflect the views of any of the granting agencies.

REFERENCES

Allsopp, H.L., Kolbe, P., 1965. Isotopic age determinations on the Cape Granite and intruded Malmesbury sediments, Cape Peninsula, South Africa. Geochimica et Cosmochimica Acta 29, 1115-1130.

Allsopp, N., Colville, J.F., Verboom, A.G. (Eds) 2014. Fynbos: ecology, evolution and conservation of a megadiverse region, Oxford University Press, Oxford.

Backeberg, N.R., Reid, D.L., Trumbull, R.B., Romer, R.L., 2011. Petrogenesis of the False Bay Dyke Swarm, Cape Peninsula, South Africa: Evidence for Basement Assimilation. South African Journal of Geology 114, 335–352. doi:10.2113/gssajg.114.3-4.335

Balasse, M., 2002. Reconstructing dietary and environmental history from enamel isotopic analysis: time resolution of intra- tooth sequential sampling. International Journal of Osteoarchaeology 12, 155–165.

Balasse, M., Ambrose, S.H., Smith, A., Price, T.D., 2002. The seasonal mobility model for prehistoric herders in the south-western Cape of South Africa assessed by isotopic analysis of sheep tooth enamel. J Archaeol Sci 29, 917–932.

Bar-Matthews, M., Marean, C.W., Jacobs, Z., Karkanas, P., Fisher, E.C., Herries, A.I.R., Brown, K., Williams, H.M., Bernatchez, J., Ayalon, A., Nilssen, P.J., 2010. A high resolution and continuous isotopic speleothem record of paleoclimate and paleoenvironment from 90 to 53 ka from Pinnacle Point on the south coast of South Africa. Quaternary Sci Rev 29, 2131–2145. doi:10.1016/j.quascirev.2010.05.009

Bataille, C.P., Laffoon, J., Bowen, G.J., 2012. Mapping multiple source effects on the strontium isotopic signatures of ecosystems from the circum-Caribbean region. Ecosphere 3, 1-24.

Bergh, N. G., et al. (2014). Vegetation types of the Greater Cape Floristic Region. Fynbos: Ecology, Evolution, and Conservation of a Megadiverse Region. N. Allsopp, J. F. Colville and T. Verboom. Oxford, Oxford University Press: 1-25.

Blum, J., Taliaferro, E., Weisse, M., Holmes, R., 2000. Changes in Sr/Ca, Ba/Ca and 87Sr/86Sr ratios between trophic levels in two forest ecosystems in the northeastern USA. Biogeochemistry 49, 87–101.

Boshoff, A.F., Kerley, G., 2001. Potential distributions of the medium- to large-sized mammals in the Cape Floristic Region, based on historical accounts and habitat requirements. African Zoology 36, 245–273.

Boshoff, A.F., Kerley, G.I.H., Cowling, R.M., 2001. A pragmatic approach to estimating the distributions and spatial requirements of the medium- to large- sized mammals in the Cape Floristic Region, South Africa. Diversity and Distributions 7, 29–43. doi:10.1046/j.1472-4642.2001.00095.x

Bradshaw, P.L. and Cowling, R.M., 2014. Landscapes, rock types, and climate of the Greater Cape Floristic Region. In: Allsopp N, Colville JF and Verboom AG (eds) Fynbos: ecology, evolution and conservation of a megadiverse region. Oxford University Press, Oxford, 26-46.

Britton, K., Grimes, V., Dau, J., Richards, M.P., 2009. Reconstructing faunal migrations using intra-tooth sampling and strontium and oxygen isotope analyses: a case study of modern caribou (*Rangifer tarandus granti*). J Archaeol Sci 36, 1163–1172. doi:10.1016/j.jas.2009.01.003

1038 Britton, K., Grimes, V., Niven, L., Steele, T.E., McPherron, S., Soressi, M., Kelly, T.E.,
1039 Jaubert, J., Hublin, J.-J., Richards, M.P., 2011. Strontium isotope evidence for
1040 migration in late Pleistocene Rangifer: Implications for Neanderthal hunting
1041 strategies at the Middle Palaeolithic site of Jonzac, France. J Hum Evol 61, 176–185.
1042 doi:10.1016/j.jhevol.2011.03.004
1043 Broad, D. S., Jungslager, E. H. A., McLachlan, I. R., Roux, J., 2006. Offshore Mesozoic
1044 Basins. In: Johnson, M. R., Annhauser, C. R. and Thomas, R. J. (Eds.), The Geology
1045 of South Africa. Geological Society of South Africa, Johannesburg/Council for
1046 Geoscience, Pretoria, 553-571.
1047 Brown, W.A.B., Christofferson, P.V., Massler, M., Weiss, M.B., 1960. Postnatal tooth
1048 development in cattle. Am. J. Vet. Res. 21, 7e34.
1049 Brown, K.S., Marean, C.W., Herries, A., Jacobs, Z., 2009. Fire as an engineering tool of
1050 early modern humans. Science 325, 859–862. doi:10.1126/science.1175028
1051 Brown, K.S., Marean, C.W., Jacobs, Z., Schoville, B.J., Oestmo, S., Fisher, E.C.,
1052 Bernatchez, J., Karkanas, P., Matthews, T., 2012. An early and enduring advanced
1053 technology originating 71,000 years ago in South Africa. Nature 491, 590–.
1054 doi:10.1038/nature11660
1055 Bryant, R.G., Bigg, G.R., Mahowald, N.M., Eckardt, F.D., Ross, S.G., 2007. Dust
1056 emission response to climate in southern Africa. Journal of Geophysical Research-
1057 Atmospheres 112. doi:10.1029/2005JD007025
1058 Budd, P., Montgomery, J., Barreiro, B., Thomas, R., 2000. Differential diagenesis of
1059 strontium in archaeological human dental tissues. Applied Geochemistry 15, 687–
1060 694.
1061 Cawthra, H.C., 2014. The marine geology of Mossel Bay. PhD Thesis, University of
1062 Cape Town, South Africa. 283 pp.
1063 Cawthra, H. C., Bateman, M. D., Carr, A. S., Compton, J. S., Holmes, P. J., 2014.
1064 Understanding Late Quaternary change at the land–ocean interface: a synthesis of the
1065 evolution of the Wilderness coastline, South Africa. . Quaternary Science Reviews
1066 99(1), 210-223.
1067 Cawthra, H.C., Compton, J. S., Fisher, E. C., Marean, C. W., (2015). Submerged
1068 shorelines and landscape features offshore of Mossel Bay, South Africa. In: Harff, J.,
1069 Bailey, G., Lüth F. (Eds.) Geology and Archaeology: Submerged landscapes of the
1070 continental shelf. *Special Publication of the Geological Society of London*, 411, 219–
1071 233. doi: 10.1144/SP411.11.
1072 Chadwick, O.A., Derry, L.A., Bern, C.R., Vitousek, P.M., 2009. Changing sources of
1073 strontium to soils and ecosystems across the Hawaiian Islands. Chemical Geology
1074 267, 64–76. doi:10.1016/j.chemgeo.2009.01.009
1075 Chase, B.M., Meadows, M.E., 2007. Late Quaternary dynamics of southern Africa's
1076 winter rainfall zone. Earth-Science Reviews 84, 103–138.
1077 doi:10.1016/j.earscirev.2007.06.002
1078 Chesson, L.A., Tipple, B.J., Mackey, G.N., Hynek, S.A., Fernandez, D.P., Ehleringer,
1079 J.R., 2012. Strontium isotopes in tap water from the coterminous USA. Ecosphere 3,
1080 art67. doi:10.1890/ES12-00122.1
1081 Chiaradia, M., Gallay, A., Todt, W., 2003. Different contamination styles of prehistoric
1082 human teeth at a Swiss necropolis (Sion, Valais) inferred from lead and strontium
1083 isotopes. Applied Geochemistry 18, 353–370.

1084 Clark, J.D., Beyene, Y., WoldeGabriel, G., Hart, W.K., Renne, P.R., Gilbert, H., Defleur,
1085 A., Suwa, G., Katoh, S., Ludwig, K.R., Boisserie, J.-R., Asfaw, B., White, T.D.,
1086 2003. Stratigraphic, chronological and behavioural contexts of Pleistocene Homo
1087 sapiens from Middle Awash, Ethiopia. Nature 423, 747–752.
1088 doi:10.1038/nature01670
1089 Compton, J.S., 2011. Pleistocene sea-level fluctuations and human evolution on the
1090 southern coastal plain of South Africa. Quaternary Sci Rev 30, 506–527.
1091 doi:10.1016/j.quascirev.2010.12.012
1092 Copeland, S., Sponheimer, M., de Ruiter, D.J., Lee-Thorp, J.A., Codron, D., le Roux,
1093 P.J., Grimes, V., Richards, M.P., 2011. Strontium isotope evidence for landscape use
1094 by early hominins. Nature 474, 76–78. doi:10.1038/nature10149
1095 Copeland, S., Sponheimer, M., Lee-Thorp, J.A., le Roux, P.J., de Ruiter, D.J., Richards,
1096 M.P., 2010. Strontium isotope ratios in fossil teeth from South Africa: assessing laser
1097 ablation MC-ICP-MS analysis and the extent of diagenesis. J Archaeol Sci 37, 1437–
1098 1446. doi:10.1038/j.jas.2010.01.003
1099 Cowling, R.M., 1983. The occurrence of C3 and C4 grasses in fynbos and allied
1100 shrublands in the South Eastern Cape, South Africa. Oecologia 58, 121–127.
1101 doi:10.1007/BF00384551
1102 Cowling, R.M., Lombard, A.T., 2002. Heterogeneity, speciation/extinction history and
1103 climate: explaining regional plant diversity patterns in the Cape Floristic Region.
1104 Diversity and Distributions 8, 163–179.
1105 Cowling, R.M., Potts, A.J., 2015. Climatic, edaphic and fire regime determinants of
1106 biome boundaries in the eastern Cape Floristic Region. South African Journal of
1107 Botany. doi:10.1016/j.sajb.2015.03.182
1108 Cowling, R.M., Proches, S., Partridge, T.C., 2009. Explaining the uniqueness of the Cape
1109 flora: Incorporating geomorphic evolution as a factor for explaining its
1110 diversification. Molecular Phylogenetics and Evolution 51, 64–74.
1111 Cronwright-Schreiner, S.C. 1925. The migratory springbucks of South Africa. T. Fisher
1112 Unwin Ltd, London.
1113 Culkin, F., Cox, R.A., 1966. Sodium, potassium, magnesium, calcium and strontium in
1114 sea water. Deep Sea Research and Oceanographic Abstracts 13, 789–804.
1115 doi:10.1016/0011-7471(76)90905-0
1116 de Villiers, S., Compton, J.S., Lavelle, M., 2000. The strontium isotope systematics of the
1117 Orange River, Southern Africa. South African Journal of Geology 103, 237–248.
1118 Dingle, R.V., Siesser, W.G., Newton, A.R., 1983. Mesozoic and Tertiary geology of
1119 southern Africa, 375 ed. Balkema, Rotterdam.
1120 Durante, C., Baschieri, C., Bertacchini, L., Cocchi, M., Sighinolfi, S., Silvestri, M.,
1121 Marchetti, A., 2013. Geographical traceability based on Sr-87/Sr-86 indicator: A first
1122 approach for PDO Lambrusco wines from Modena. Food Chemistry 141, 2779–
1123 2787. doi:10.1016/j.foodchem.2013.05.108
1124 Ericson, J.E., 1985. Strontium isotope characterization in the study of prehistoric human
1125 ecology. J Hum Evol 14, 503–514. doi:10.1016/S0047-2484(85)80029-4
1126 Estes, R.D., 1991. The behavior guide to African mammals. University of California
1127 Press, Berkeley.
1128 Evans, J.A., Montgomery, J., Wildman, G., 2009. Isotope domain mapping of 87Sr/86Sr
1129 biosphere variation on the Isle of Skye, Scotland. Journal of the Geological Society

166, 617-631. doi:10.1144/0016-76492008-043.
Evans, J.A., Montgomery, J., Wildman, G., Boulton, N., 2010. Spatial variations in biosphere 87Sr/86Sr in Britain. Journal of the Geological Society 167, 1–4. doi:10.1144/0016-76492009-090
Faith, J.T., 2013. Taphonomic and paleoecological change in the large mammal sequence from Boomplaas Cave, western Cape, South Africa. J Hum Evol 65, 715–730. doi:10.1016/j.jhevol.2013.09.001
Faith, J.T., Thompson, J.C., 2013. Fossil evidence for seasonal calving and migration of extinct blue antelope (Hippotragus leucophaeus) in southern Africa. J Biogeogr 40, 2108–2118. doi:10.1111/jbi.12154
Fenner, J.N., Wright, L.E., 2014. Revisiting the strontium contribution of sea salt in the human diet. J Archaeol Sci 44, 99–103. doi:10.1016/j.jas.2014.01.020
Fisher, E.C., Bar-Matthews, M., Jerardino, A., Marean, C.W., 2010. Middle and Late Pleistocene paleoscape modeling along the southern coast of South Africa. Quaternary Sci Rev 29, 1382–1398. doi:10.1016/j.quascirev.2010.01.015
Franklin, J., Potts, A.J., Fisher, E.C., Cowling, R.M., Marean, C.W., 2015. Paleodistribution modeling in archaeology and paleoanthropology. Quaternary Sci Rev 110, 1–14. doi:10.1016/j.quascirev.2014.12.015
Gadbury, C., Todd, L., Jahren, A.H., Amundson, R., 2000. Spatial and temporal variations in the isotopic composition of bison tooth enamel from the Early Holocene Hudson–Meng Bone Bed, Nebraska. Palaeogeography, Palaeoclimatology, Palaeoecology 157, 79-93. doi:10.1016/S0031-0182(99)00151-0
Gage, J.P., Francis, M.J.O., Triffit, J.T., 1989. Collagen and Dental Matrices. Butter-worth-Heinemann, London.
Goldblatt, P., Manning, J.C., 2002. Plant diversity of the Cape region of southern Africa. Annals of the Missouri Botanical Garden 281–302.
Gonder, M.K., Mortensen, H.M., Reed, F.A., de Sousa, A., Tishkoff, S.A., 2007. Whole-mtDNA Genome Sequence Analysis of Ancient African Lineages. Molec.Bio.Evol. 24, 757–768.
Hälbich, I.W., 1983. A geodynamic model for the Cape Fold Belt. In Söhnge, A. P. G and Hälbich, I. W. (Eds.) Geodynamics of the Cape fold Belt Special Publication of the Geological Society of South Africa 12, 177-184.
Hartman, G., Richards, M., 2014. Mapping and defining sources of variability in bioavailable strontium isotope ratios in the Eastern Mediterranean. Geochimica et Cosmochimica Acta 126, 250–264. doi:10.1016/j.gca.2013.11.015
Henn, B.M., Gignoux, C.R., Jobin, M., Granka, J.M., Macpherson, J.M., Kidd, J.M., Rodriguez-Botigue, L., Ramachandran, S., Hon, L., Brisbin, A., Lin, A.A., Underhill, P.A., Comas, D., Kidd, K.K., Norman, P.J., Parham, P., Bustamante, C.D., Mountain, J.L., Feldman, M.W., 2011. Hunter-gatherer genomic diversity suggests a southern African origin for modern humans. Proceedings of the National Academy of Sciences of the United States of America 108, 5154–5162. doi:10.1073/pnas.1017511108
Hoppe, K., Koch, P., 2007. Reconstructing the migration patterns of late Pleistocene mammals from northern Florida, USA. Quaternary Research 68, 347–352.
Hoppe, K., Koch, P., Furutani, T., 2003. Assessing the preservation of biogenic strontium in fossil bones and tooth enamel. International Journal of Osteoarchaeology 13, 20–28.

1176 Hoppe, K.A., Stover, S.M., Pascoe, J.R., Amundson, R., 2004. Tooth enamel
1177 biomineralization in extant horses: implications for isotopic microsampling.
1178 Palaeogeography, Palaeoclimatology, Palaeoecology 206, 355–365.
1179 doi:10.1016/j.palaeo.2004.01.012
1180 Horne, R.A., 1969. Marine chemistry; the structure of water and the chemistry of the
1181 hydrosphere. Wiley-Interscience.
1182 Jacobs, Z., 2010. An OSL chronology for the sedimentary deposits from Pinnacle Point
1183 Cave 13B--A punctuated presence. J Hum Evol 59, 289–305.
1184 Janney, P.E., Roex, A.P.L., Carlson, R.W., Viljoen, K.S., 2002. A Chemical and Multi-
1185 Isotope Study of the Western Cape Olivine Melilitite Province, South Africa:
1186 Implications for the Sources of Kimberlites and the Origin of the HIMU Signature in
1187 Africa. Journal of Petrology 43, 2339–2370. doi:10.1093/petrology/43.12.2339
1188 Johnson, H. D., Baldwin, C. T. 1986. Shallow siliciclastic seas. In: Reading, H. G. (Ed.),
1189 Sedimentary environments and facies. Second Edition. Blackwell Scientific
1190 Publications, Oxford, pp. 229-282.
1191 Johnson, M.R., van Vuuren, C.J., Visser, J.N.J., Cole, D.I., Wickens, de V., Christie,
1192 A.D.M., Roberts, D.L., Brandl, G., 2006. Sedimentary rocks of the Karoo
1193 Supergroup. In: M.R. Johnson, C.R., Annhauser, R.J. Thomas (Eds.), The Geology
1194 of South Africa. Geological Society of South Africa/Council for Geoscience Pretoria,
1195 461-501.
1196 Julien, M.-A., Bocherens, H., Burke, A., Drucker, D.G., Patou-Mathis, M., Krotova, O.,
1197 Péan, S., 2012. Were European steppe bison migratory? 18O, 13C and Sr intra-tooth
1198 isotopic variations applied to a palaeoethological reconstruction. Quaternary
1199 International 271, 106–119. doi:10.1016/j.quaint.2012.06.011
1200 Karkanas, P., Goldberg, P., 2010. Site formation processes at Pinnacle point Cave 13B
1201 (Mossel Bay, Western Cape Province, South Africa): resolving stratigraphic and
1202 depositional complexities with micromorphology. J Hum Evol 59, 256–273.
1203 doi:10.1016/j.jhevol.2010.07.001
1204 Kelly RL. 1995. *The Foraging Spectrum*. Washington D.C.: Smithsonian Institution
1205 Press
1206 Klein, R.G., 1994. The Long-Horned African Buffalo (Pelorovis antiquus) is an Extinct
1207 Species. J Archaeol Sci 21, 725–733. doi:10.1006/jasc.1994.1072
1208 Klein, R.G., 1983. Palaeoenvironmental implications of Quaternary large mammals in the
1209 Fynbos Region, in: Deacon, H.J., Hendey, Q.B., Lambrechts, J.J.N. (Eds.), Fynbos
1210 Palaeoecology: a Preliminary Synthesis. Cooperative Scientific Programmes,
1211 Pretoria, pp. 116–138.
1212 Lee-Thorp, J., Sponheimer, M., 2003. Three case studies used to reassess the reliability of
1213 fossil bone and enamel isotope signals for paleodietary studies. Journal of
1214 Anthropological Archaeology 22, 208–216.
1215 Lutjeharms, J.R.E., 2006. The Agulhas Current. Springer-Verlag, New York.
1216 Lutjeharms, J.R.E., Monteiro, P.M.S., Tyson, P.D., Obura, D., 2001. The oceans around
1217 southern Africa and regional effects of global change. South African Journal of
1218 Science 97, 119–130.
1219 Malan, J.A., 1990. The stratigraphy and sedimentology of the Bredasdorp Group,
1220 southern Cape Province. University of Cape Town.
1221 Marean, C.W., 2014. The origins and significance of coastal resource use in Africa and

Western Eurasia. J Hum Evol 77, 17–40. doi:10.1016/j.jhevol.2014.02.025
Marean, C.W., 2011. Coastal South Africa and the co-evolution of the modern human lineage and coastal adaptations, in: Bicho, N., Haws, J.A., Davis, L.G. (Eds.), Trekking the Shore: Changing Coastlines and the Antiquity of Coastal Settlement. Springer, New York, pp. 421–440.
Marean, C.W., 2010. Pinnacle Point Cave 13B (Western Cape Province, South Africa) in context: The Cape Floral kingdom, shellfish, and modern human origins. J Hum Evol 59, 425–443. doi:10.1016/j.jhevol.2010.07.011
Marean, C.W., Anderson, R.J., Bar-Matthews, M., Braun, K., Cawthra, H.C., Cowling, R.M., Engelbrecht, F., Esler, K.J., Fisher, E., Franklin, J., Hill, K., Janssen, M., Potts, A.J., Zahn, R., 2015. A new research strategy for integrating studies of paleoclimate, paleoenvironment, and paleoanthropology. Evol. Anthropol. 24, 62–72. doi:10.1002/evan.21443
Marean, C.W., Bar-Matthews, M., Bernatchez, J., Fisher, E., Goldberg, P., Herries, A.I.R., Jacobs, Z., Jerardino, A., Karkanas, P., Minichillo, T., Nilssen, P.J., Thompson, E., Watts, I., Williams, H.M., 2007. Early human use of marine resources and pigment in South Africa during the Middle Pleistocene. Nature 449, 905–908. doi:10.1038/nature06204
Marean, C.W., Bar-Matthews, M., Fisher, E., Goldberg, P., Herries, A., Karkanas, P., Nilssen, P.J., Thompson, E., 2010. The stratigraphy of the Middle Stone Age sediments at Pinnacle Point Cave 13B (Mossel Bay, Western Cape Province, South Africa). J Hum Evol 59, 234–255. doi:10.1016/j.jhevol.2010.07.007
Marean, C.W., Cawthra, H.C., Cowling, R.M., 2014. Stone age people in a changing South African greater Cape Floristic Region, in: Allsopp, N., Colville, J.F., Verboom, T. (Eds.), Fynbos. Ecology, Evolution, and Conservation of a Megadiverse Region, Ecology, Evolution, and Conservation of a Megadiverse Region. Oxford University Press, pp. 164–199. doi:10.1093/acprof:oso/9780199679584.003.0008
Marlowe, F.W., 2005. Hunter- gatherers and human evolution. Evol. Anthropol. 14, 54–67. doi:10.1002/evan.20046
Martin, A.K., Flemming, B.W., 1986. The Holocene shelf sediment wedge off the south and east coast of South Africa. In: Knight, R.J. & McLean, J.R. (eds) Shelf Sands and Sandstones. Canadian Society of Petroleum Geologists Memoir 2, 27–44.
Martin, A.K., Hartnady, C.J.H., 1986. Plate tectonic development of the southeast Indian Ocean: A revised reconstruction of East Antarctica and Africa. Journal of Geophyiscal Research 91, 4767-4786.
Maurer, A.-F., Galer, S.J.G., Knipper, C., Beierlein, L., Nunn, E.V., Peters, D., Tütken, T., Alt, K.W., Schöne, B.R., 2012. Bioavailable 87Sr/86Sr in different environmental samples — Effects of anthropogenic contamination and implications for isoscapes in past migration studies. Science of the Total Environment 433, 216–229. doi:10.1016/j.scitotenv.2012.06.046
McDougall, I., Brown, F.H., Fleagle, J.G., 2005. Stratigraphic placement and age of modern humans from Kibish, Ethiopia. Nature 433, 733–736.
Midgley, J.J., Harris, C., Harington, A., Potts, A.J., 2012. Geochemical perspective on origins and consequences of heuweltjie formation in the Southwestern Cape, South Africa. South African Journal of Geology 115, 577-588. doi:10.2113/gssajg.115.4
Milani, E.J., de Wit, M.J., 2008. Correlations between classic Parana and Cape-Karoo

basins of South America and southern Africa and their basin infills flanking the Gondwanides: Du Toit revisited. InWest Gondwana: Pre-Cenozoic Correlations Across the South Atlantic Region. In: Pankhurst, R.J., Trouw, R.A.J., de Brito Neves, B.B., de Wit, M.J (Eds.), Geological Society, London, Special Publication, 294, pp. 319–342.

Mills MGL. 1990. Kalahari Hyaenas: The Comparative Behavioural Ecology of Two Species, . Unwin Hyman, London

Montgomery, J., 2010. Passports from the past: Investigating human dispersals using strontium isotope analysis of tooth enamel. Annals of human biology 37, 325-346. doi: 10.3109/03014461003649297

Montgomery, J., Evans, J.A., Horstwood, M.S.A., 2010. Evidence for long-term averaging of strontium in bovine enamel using TIMS and LA-MC-ICP-MS strontium isotope intra-molar profiles. Environmental Archaeology 15, 32–42. doi:10.1179/146141010X12640787648694

Montgomery, J., Evans, J.A., Wildman, G., 2006. Sr-87/Sr-86 isotope composition of bottled British mineral waters for environmental and forensic purposes. Applied Geochemistry 21, 1626–1634. doi:10.1016/j.apgeochem.2006.07.002

Myers, N., Mittermeier, R.A., Mittermeier, C.G., da Fonseca, G.A.B., Kent, J., 2000. Biodiversity hotspots for conservation priorities. Nature 403, 853–858.

Odum, H.T., 1957. Strontium in natural waters. Publ. Inst. Mar. Sci. Univ. Texas IV (2).

Parker, R.J., Siesser, W.G., 1972. Petrology and origin of some phosphorites from the South African continental margin. Journal of Sedimentary Research 42, 434–440.

Paton, D.A., Macdonald, D.I.M., Underhill, J.R., 2006. Applicability of thin or thick skinned structural models in a region of multiple inversion episodes, southern. South African Journal of Structural Geology 28, 1933-1947.

Passey, B., Cerling, T., 2002. Tooth enamel mineralization in ungulates: implications for recovering a primary isotopic time-series. Geochimica et Cosmochimica Acta 66, 3225–3234.

Pellegrini M., R.E. Donahue, C. Chenery, J. Evans, J.A Lee-Thorp, J. Montgomery, M. Mussi. 2008. Faunal migration in late-glacial central Italy: implications for human resource exploitation. Rapid Comm. Mass Spectrom. 22: 1714–1726.

Petit, J.R., Jouzel, J., Raynaud, D., Barkov, N.I., Barnola, J.M., Basile, I., Bender, M., Chappellaz, J., Davis, M., Delaygue, G., Delmotte, M., Kotlyakov, V.M., Legrand, M., Lipenkov, V.Y., Lorius, C., Pepin, L., Ritz, C., Saltzman, E., Stievenard, M., 1999. Climate and atmospheric history of the past 420,000 years from the Vostok ice core, Antarctica. Nature 399, 429–436.

Pickrell, J.K., Patterson, N., Barbieri, C., Berthold, F., Gerlach, L., Guldemann, T., Kure, B., Mpoloka, S.W., Nakagawa, H., Naumann, C., Lipson, M., Loh, P.-R., Lachance, J., Mountain, J., Bustamante, C.D., Berger, B., Tishkoff, S.A., Henn, B.M., Stoneking, M., Reich, D., Pakendorf, B., 2012. The genetic prehistory of southern Africa. Nat Commun 3, 1143. doi:10.1038/ncomms2140

Pin, C., Briot D., Bassin C. and Poitrasson F. 1994. Concomitant separation of strontium and samarium-neodymium for isotopic analysis in silicate samples, based on specific extraction chromatography. Anal. Chim. Acta 298, 209-217.

Poszwa, A., Ferry, B., Pollie, B., Grimaldi, C., Charles-Dominique, P., Loubet, M., Dambrine, E., 2009. Variations of plant and Soil Sr-87/Sr-86 along the slope of a

tropical inselberg. Ann Forest Sci 66, –. doi:10.1051/forest/2009036
Price, T.D., Johnson, C., Ezzo, J., Burton, J., Ericson, J., 1994. Residential mobility in the prehistoric southwest United States: a preliminary study using strontium isotope analysis. J Archaeol Sci 21, 315–315.
Price, T.D., Meiggs, D., Weber, M.J., Pike-Tay, A., 2015. The migration of Late Pleistocene reindeer: isotopic evidence from northern Europe. Archaeol Anthropol Sci. doi:10.1007/s12520-015-0290-z
Radloff, F., Mucina, L., Bond, W.J., Roux, P.J., 2010. Strontium isotope analyses of large herbivore habitat use in the Cape Fynbos region of South Africa. Oecologia 164, 567–578. doi:10.1007/s00442-010-1731-0
Rautenbach, I.L., 1971. Ageing criteria in the springbok, Antidorcas Marsupialis (Zimmermann, 1780) (Artiodactyla: Bovidae). Annals of the Transvaal Museum 27, 83–133.
Rector, A., Reed, K.E., 2010. Middle and late Pleistocene faunas of Pinnacle Point and their paleoecological implications. J Hum Evol 59, 340–357. doi:10.1016/j.jhevol.2010.07.002
Roberts, D.L., Cawthra, H.C., Musekiwa, C., 2013. Dynamics of late Cenozoic aeolian deposition along the South African coast: A record of evolving climate and ecosystems. In: Martini, I. P., Wanless, H. R. (Eds.), Sedimentary Coastal Zones from High to Low Latitudes: Similarities and Differences. Geological Society, London, Special Publications 388.
Rogers, J., 1971a. Quaternary sediments of the Agulhus Bank, Cape Point to Cape St. Francis, in: Sancor Technical Report No. 3. Department of Geology, University of Cape Town, Cape Town.
Rogers, J., 1971b. Sedimentology of Quaternary deposits on the Agulhas Bank. University of Cape Town.
Rozendaal, A., Gresse, P.G., Scheepers, R., Le Roux, J.P., 1999. Neoproterozoic to Early Cambrian crustal evolution of the Pan-African Saldania Belt, South Africa. Precambrian Research 97 (3–4), 303–323.
Schlebusch, C.M., Skoglund, P., Sjöin, P., attepaille, L.M., ernandez, D., ay, F., i, S., e Jongh, M., ingleton, A., lum, M.G.B., oodyall, H., akobsson, M., 2012. Genomic Variation in Seven Khoe-San Groups Reveals Adaptation and Complex African History. Science 338, 374–379.
Schulze, B.R., 1972. South Africa, in: Griffiths, J.F. (Ed.), Climates of Africa. World Survey of Climatology, Vol. 10. Elsevier, Amsterdam, pp. 501–566.
Sealy, J., 1996. Seasonality of rainfall around the Last Glacial Maximum as reconstructed from carbon isotope analyses of animal bones from Nelson Bay Cave. South African Journal of Science 92, 441–444.
Sealy, J., van der Merwe, N., Sillen, A., 1991. 87Sr/86Sr as a dietary indicator in modern and archaeological bone. Journal of Archaeological Science 18, 399-416.
Sillen, A., Hall, G., Richardson, S., Armstrong, R., 1998. 87Sr/86Sr ratios in modern and fossil food-webs of the Sterkfontein Valley: implications for early hominid habitat preference. Geochimica et Cosmochimica Acta. 62, 2463-2473.
Skead, C. J. (2011). Historical incidence of the larger land mammals in the broader Western and Northern Cape. Port Elizabeth, Nelson Mandela Metropolitan University.

Skinner, J. D. & Smithers, R. H. N., 1990. *The Mammals of the Southern African Subregion*. Pretoria: University of Pretoria.
Soderberg, K., Compton, J.S., 2007. Dust as a nutrient source for fynbos ecosystems, South Africa. Ecosystems 10, 550–561. doi:10.1007/s10021-007-9032-0
Thamm, A.G., Johnson, M.R., 2006. The Cape Supergroup. In: Johnson, M. R., Annhauser, C. R. and Thomas, R. J. (Eds.), The Geology of South Africa. Geological Society of South Africa, Johannesburg/Council for Geoscience Pretoria, 443-461.
Thompson, J.C., 2010. Taphonomic analysis of the Middle Stone Age faunal assemblage from Pinnacle Point Cave 13B, Western Cape, South Africa. J Hum Evol 59, 321–339.
Thwaites & Cowling 1988. Soil-vegetation relationships on the Agulhas Plain, South Africa. Catena 15: 333-345.
Tinker, J.H., de Wit, M.J., Brown, R.W., 2008. Linking source and sink: evaluating the balance between onshore erosion and offshore sediment accumulation since Gondwana break-up, South Africa. Tectonophysics 455, 94–103.
Van Andel, T.H., 1989. Late Pleistocene Sea Levels and the Human Exploitation of the Shore and Shelf of Southern South Africa. Journal of Field Archaeology 16, 133–155.
Vickery, K.J., Eckardt, F.D., Bryant, R.G., 2013. A sub-basin scale dust plume source frequency inventory for southern Africa, 2005-2008. Geophys. Res. Lett. 40, 5274–5279. doi:10.1002/grl.50968
Vlok, J.H.J., D.I.W. Euston-Brown, R.M. Cowling. 2003. Acocks' Valley Bushveld 50 years on: new perspectives on the delimitation, characterization and origin of subtropical thicket vegetation. South African Journal of Botany 69, 27-51.
Voerkelius, S., Lorenz, G.D., Rummel, S., Quétel, C.R., Heiss, G., Baxter, M., Brach-Papa, C., Deters-Itzelsberger, P., Hoelzl, S., Hoogewerff, J., Ponzevera, E., Van Bocxstaele, M., Ueckermann, H., 2010. Strontium isotopic signatures of natural mineral waters, the reference to a simple geological map and its potential for authentication of food. Food Chemistry 118, 933–940. doi:10.1016/j.foodchem.2009.04.125
Vogel, J.C., Fuls, A., Ellis, R.P., 1978. The geographical distribution of Kranz grasses in South Africa. South African Journal of Science 74, 209–215.
Warham, J.O., 2011. Mapping biosphere strontium isotope ratios across major lithological boundaries: a systematic investigation of the major influences on geographic variation in the 87Sr/86Sr composition of bioavailable strontium above the Cretaceous and Jurassic rocks of England. Ph.D. thesis. University of Bradford.
Watkeys, M.K., 2006. Gondwana break-up: A South African perspective. In: Johnson, M. R., Annhauser, C. R. and Thomas, R. J. (Eds.), The Geology of South Africa. Geological Society of South Africa, Johannesburg/Council for Geoscience Pretoria, 531-539.
Whipkey, C., Capo, R., Chadwick, O., Stewart, B., 2000. The importance of sea spray to the cation budget of a coastal Hawaiian soil: a strontium isotope approach. Chemical Geology 168, 37–48.
Zazzo, A., Balasse, M., 2005. High-resolution $\delta^{13}C$ intratooth profiles in bovine enamel: Implications for mineralization pattern and isotopic attenuation. Geochimica et Cosmochimica Acta 69, 3631-3642. doi:10.1016/j.gca.2005.02.031

1406 Zazzo, A., Balasse, M., Passey, B., Moloney, A.P., Monahan, F.J., Schmidt, O. 2010. The
1407 isotope record of short- and long-term dietary changes in sheep tooth enamel:
1408 Implications for quantitative reconstruction of paleodiets. Geochimica et
1409 Cosmochimica Acta 74, 3571-3586.
1410

Figure 1. Map of southern Africa showing the extent of the Greater Cape Floristic Region with important cities (inset) and Middle Stone Age/Late Stone Age archaeological sites.

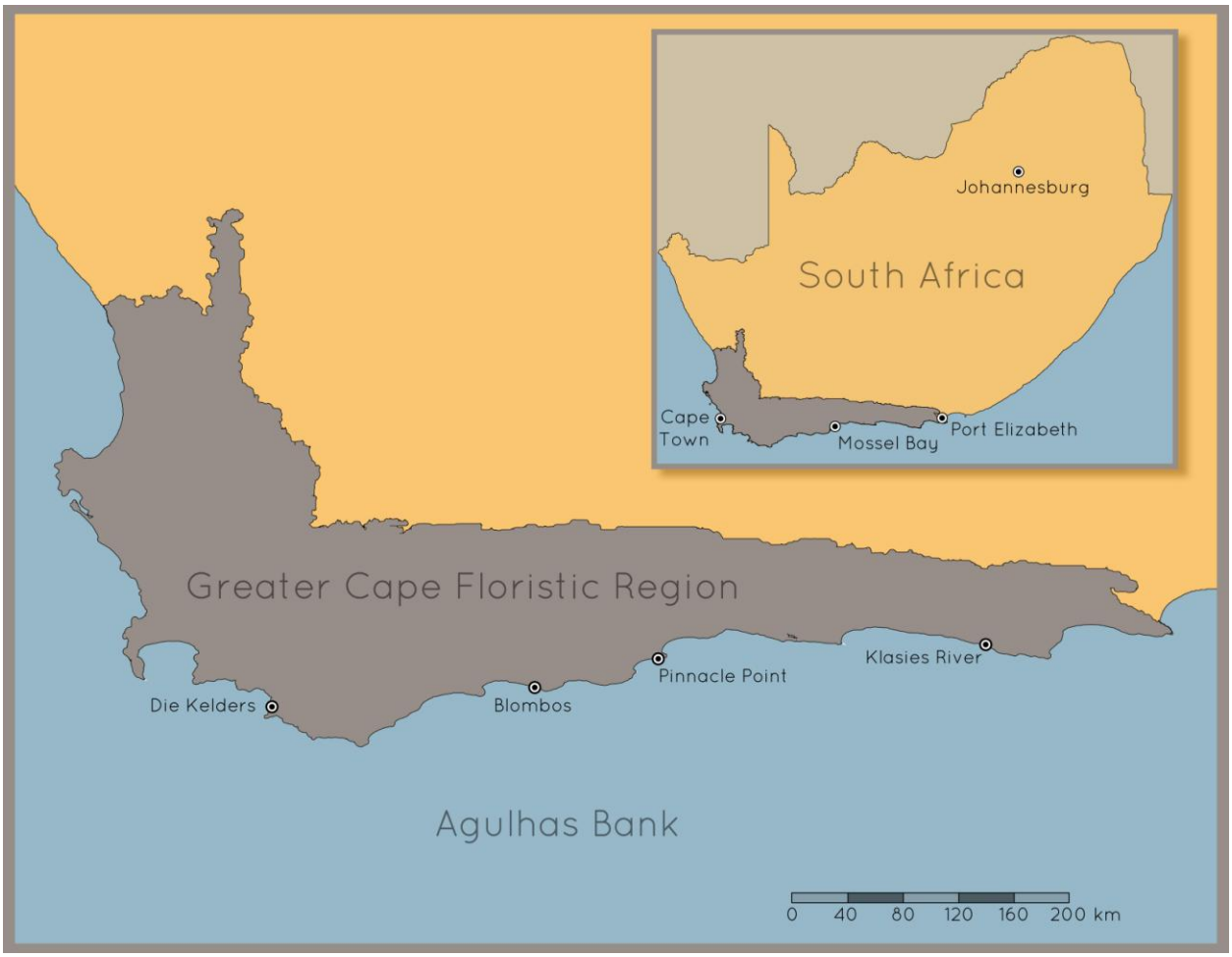

Figure 2. Map of the South African Coast showing bedrock geology, the modern coastline (solid black line), and the extent of the 151 ka shoreline (the time of PP30 fossil accumulation, dashed black line). Black dots show sampling localities at which plants were collected for biologically available $^{87}Sr/^{86}Sr$. Red dots indicate modern cities and archaeological sites.

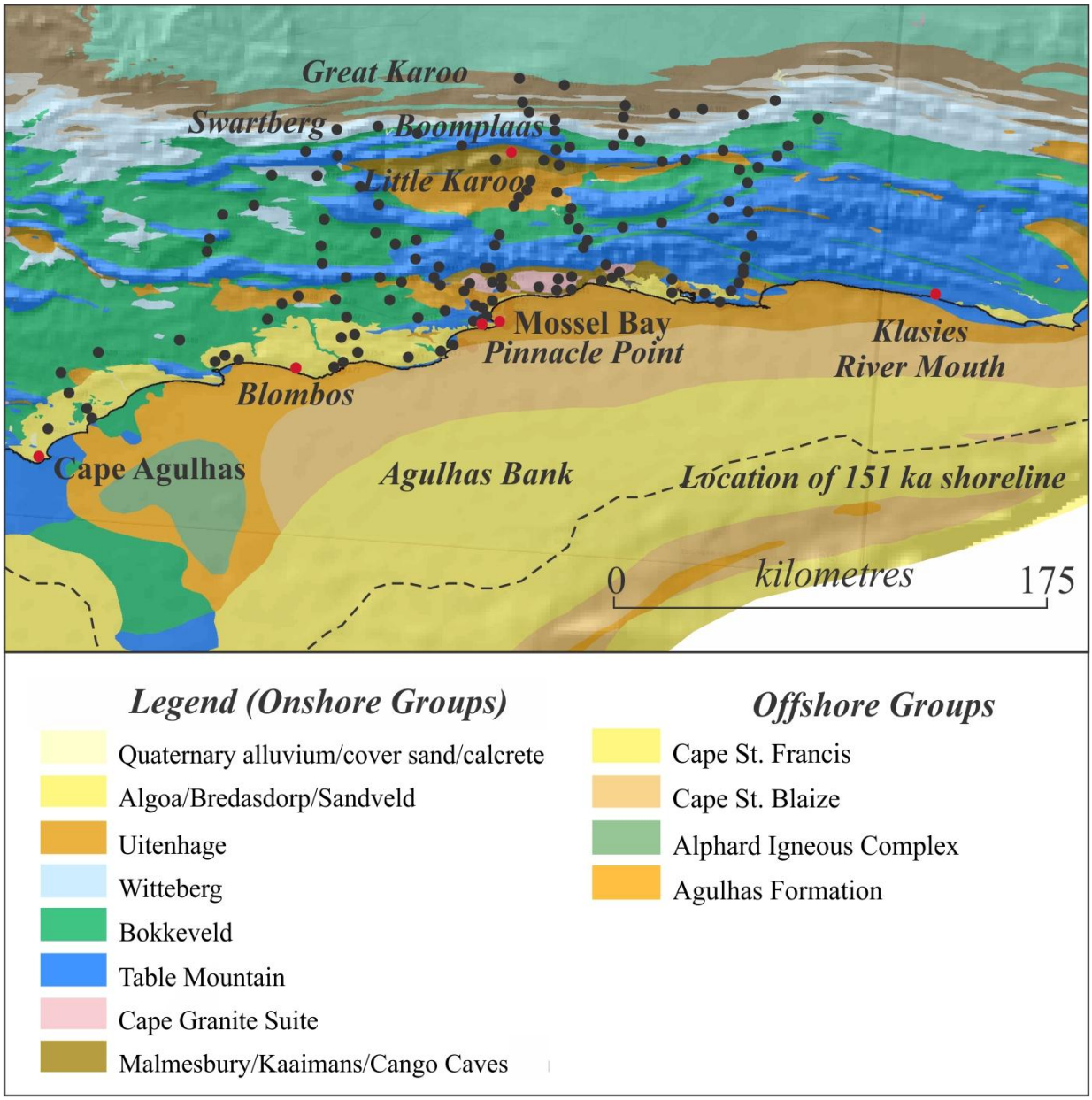

Figure 3. $^{87}Sr/^{86}Sr$ of intra- and inter-tooth samples from fossil teeth at PP13B and PP30. The legend shows the specimen number. M1, M2, M3, P4, andM1/M2 refer to the tooth. D = dentine sample. The x-axis is cumulative distance from neck, which anchors the distance of samples from the neck of the earliest forming tooth of the specimens sampled (see text for details).

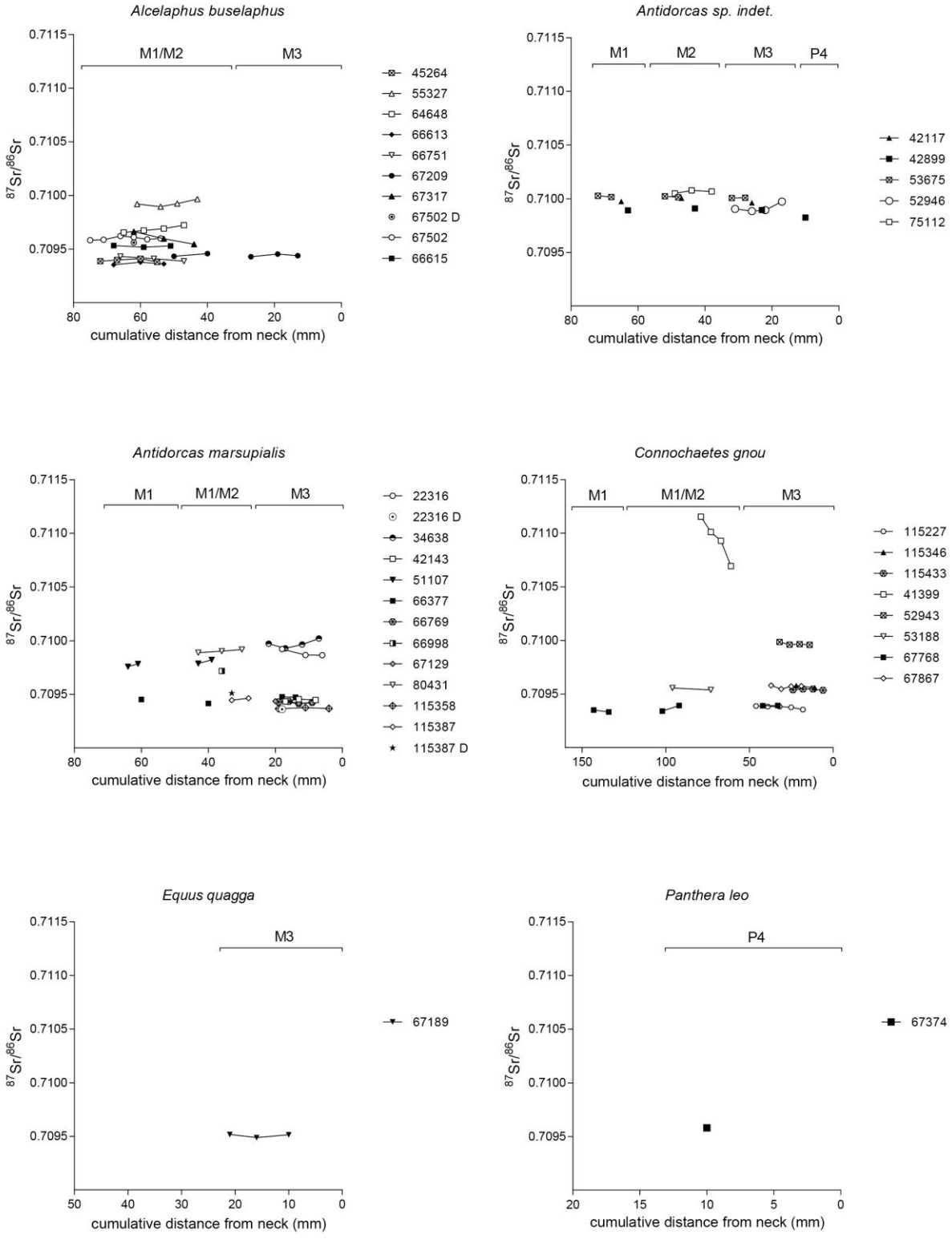
Alcelaphus buselaphus
M1/M2
M3
45264
55327
64648
66613
66751
67209
67317
67502 D
67502
66615
Antidorcas sp. indet.
M1
M2
M3
P4
42117
42899
53675
52946
75112
Antidorcas marsupialis
M1
M1/M2
M3
22316
22316 D
34638
42143
51107
66377
66769
66998
67129
80431
115358
115387
115387 D
Connochaetes gnou
M1
M1/M2
M3
115227
115346
115433
41399
52943
53188
67768
67867
Equus quagga
M3
67189
Panthera leo
P4
67374
$^{87}Sr/^{86}Sr$
cumulative distance from neck (mm)

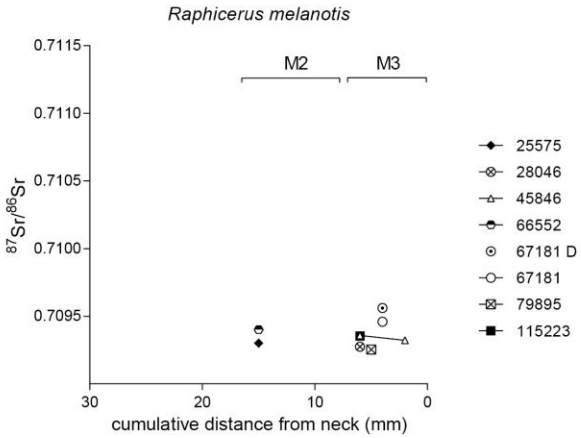
Raphicerus melanotis
M2
M3
0.7115
0.7110
0.7105
0.7100
0.7095
$^{87}Sr/^{86}Sr$
30
20
10
0
cumulative distance from neck (mm)
25575
28046
45846
66552
67181 D
67181
79895
115223

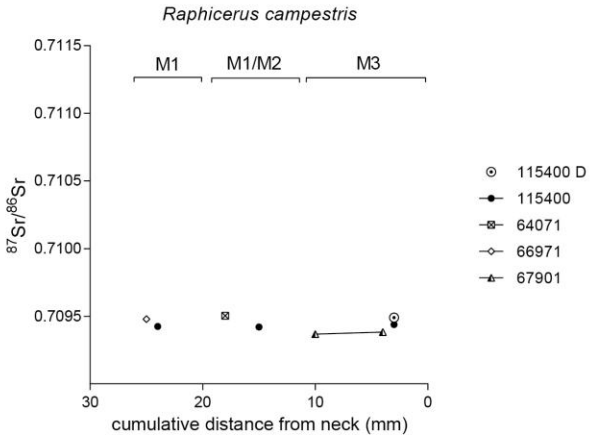
Raphicerus campestris
M1
M1/M2
M3
0.7115
0.7110
0.7105
0.7100
0.7095
$^{87}Sr/^{86}Sr$
30
20
10
0
cumulative distance from neck (mm)
115400 D
115400
64071
66971
67901

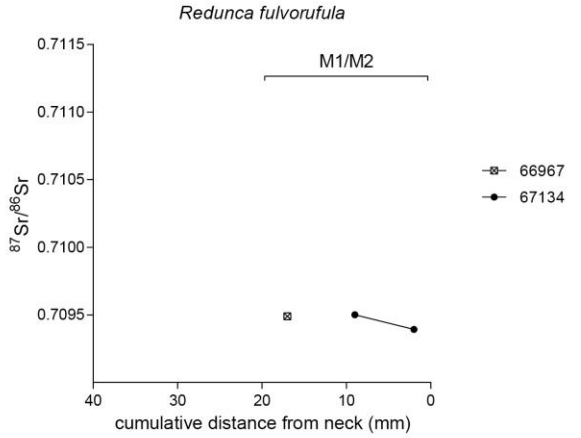
Redunca fulvorufula
M1/M2
0.7115
0.7110
0.7105
0.7100
0.7095
$^{87}Sr/^{86}Sr$
40
30
20
10
0
cumulative distance from neck (mm)
66967
67134

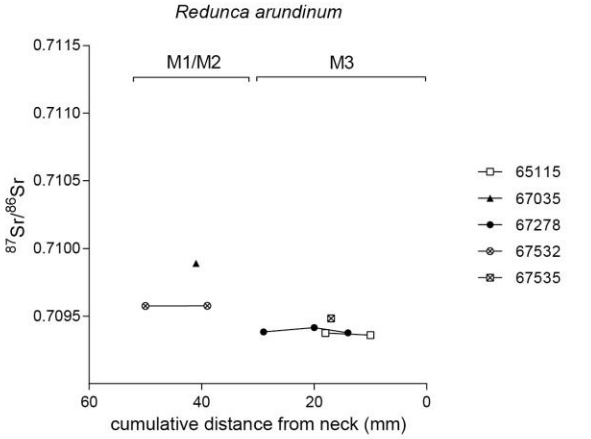
Redunca arundinum
M1/M2
M3
0.7115
0.7110
0.7105
0.7100
0.7095
$^{87}Sr/^{86}Sr$
60
40
20
0
cumulative distance from neck (mm)
65115
67035
67278
67532
67535

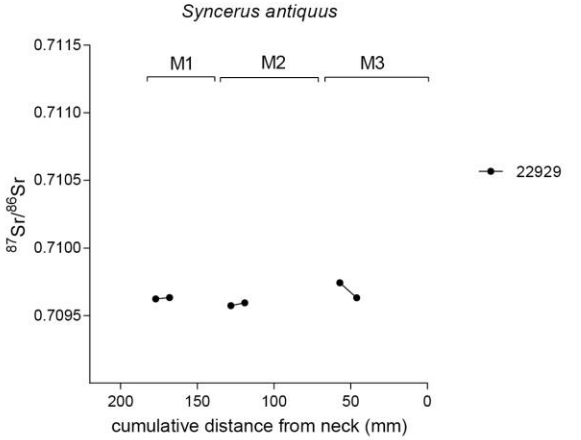
Syncerus antiquus
M1
M2
M3
0.7115
0.7110
0.7105
0.7100
0.7095
$^{87}Sr/^{86}Sr$
200
150
100
50
0
cumulative distance from neck (mm)
22929

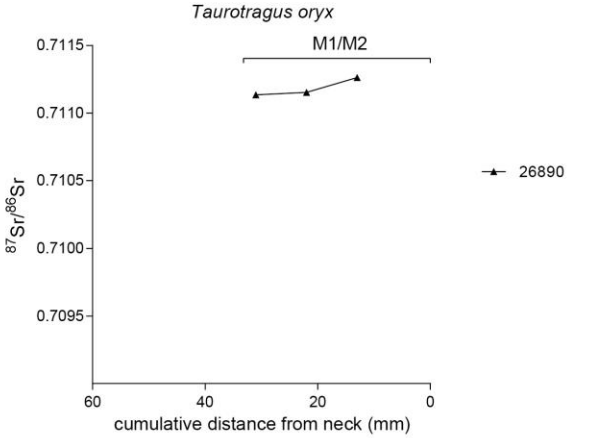
Taurotragus oryx
M1/M2
0.7115
0.7110
0.7105
0.7100
0.7095
$^{87}Sr/^{86}Sr$
60
40
20
0
cumulative distance from neck (mm)
26890

Figure 4. $^{87}Sr/^{86}Sr$ of fossil tooth enamel from PP13B and PP30 and bioavailable $^{87}Sr/^{86}Sr$ as measured by plants across the modern landscape. Plants are grouped according to the geological group of the bedrock at the sampling locality. Boxes show the median value and 25th and 75th quartiles, whiskers extend by 1.5 times the interquartile range, and all outliers are shown.

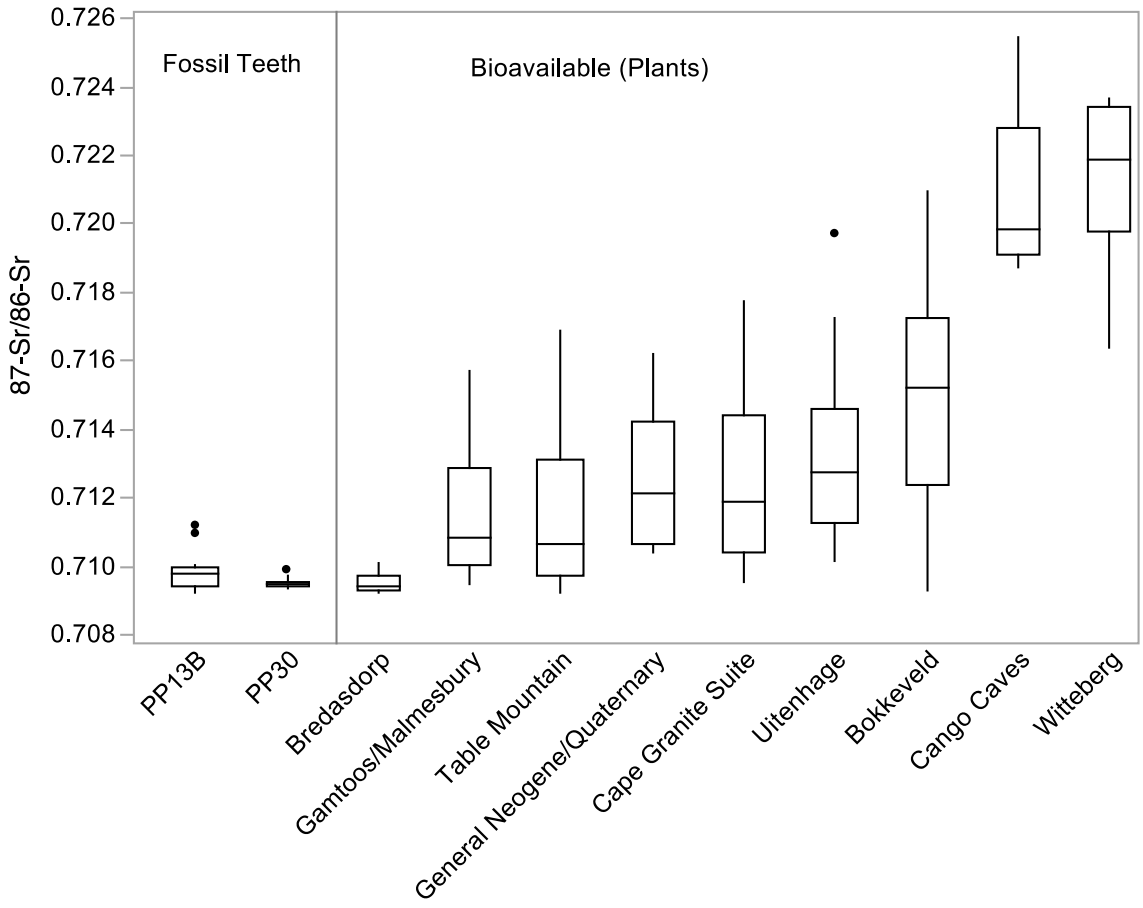

Figure 5. Bioavailable $^{87}Sr/^{86}Sr$ from the modern sampling localities plotted relative to distance to the modern coastline, latitude, and longitude.

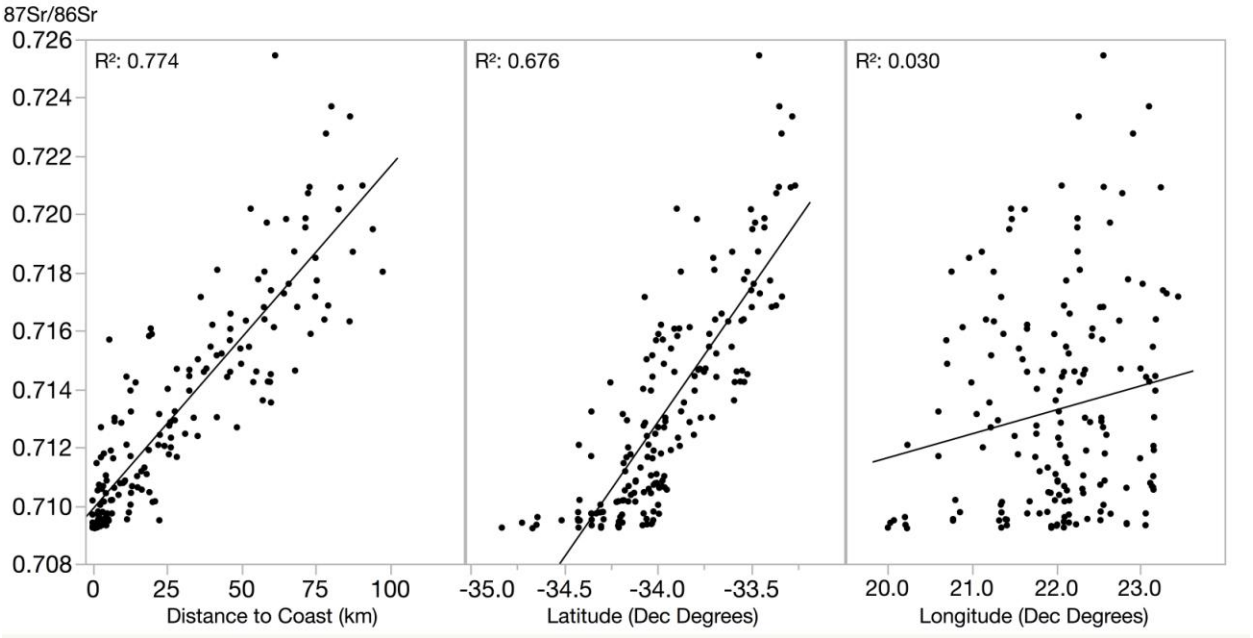

Figure 6. Bioavailable strontium isoscape ($^{87}Sr/^{86}Sr$) predictive geospatial model developed in ESRI ArcGIS 10.3. Circles with black dots in the center represent bioavailable $^{87}Sr/^{86}Sr$ sampling localities used to create the model. White dots represent the 26 randomly selected sampling locations that were extracted prior to model development and used later to test the model predictions. The size of the white dots shows the amount by which measured $^{87}Sr/^{86}Sr$ differed from the model's predictions. Contour lines show the predicted bioavailable $^{87}Sr/^{86}Sr$ based on the model. Colors indicate areas of lowest bioavailable $^{87}Sr/^{86}Sr$ (blue) to highest bioavailable $^{87}Sr/^{86}Sr$ (red).

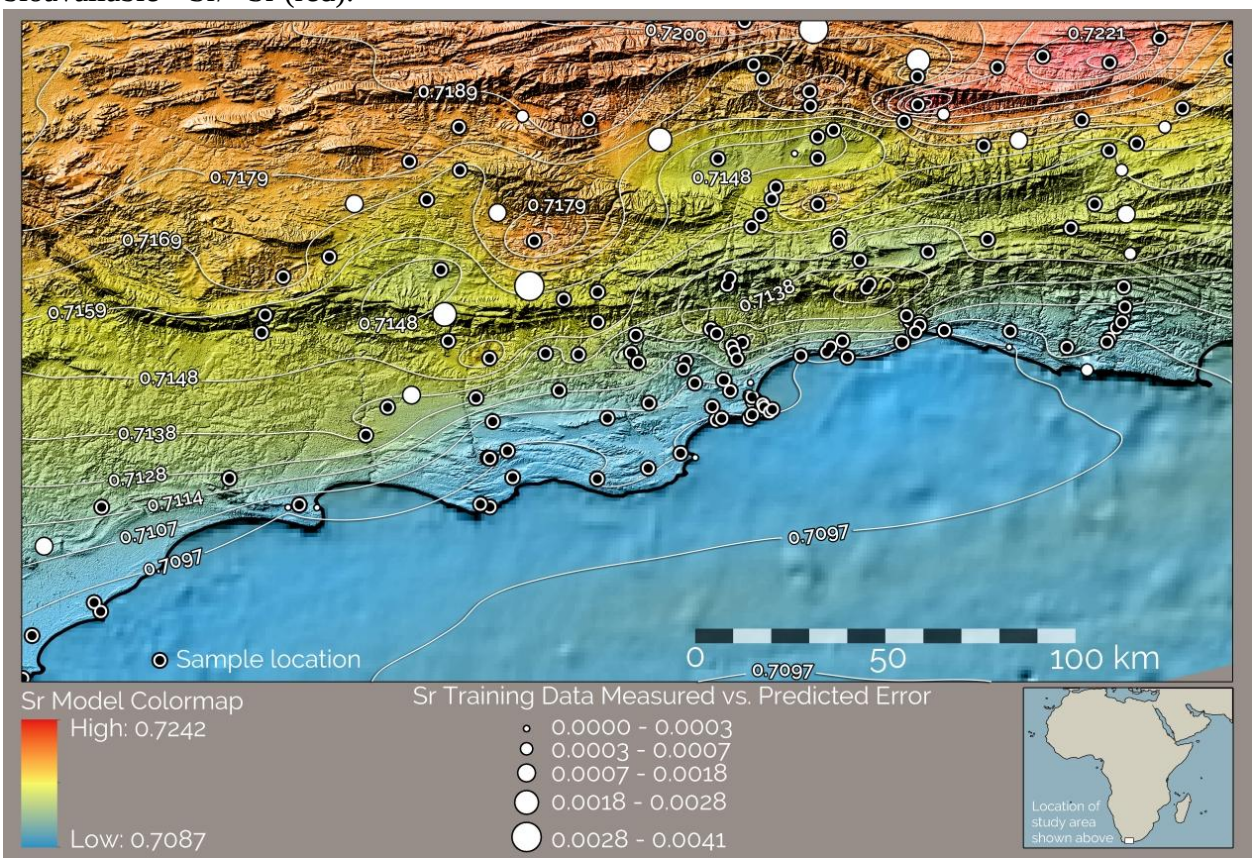

Figure 7. Results of fossil enamel samples by genus and site. Each point represents the average of all intra- and inter-tooth samples from one specimen as reported in Table 1.

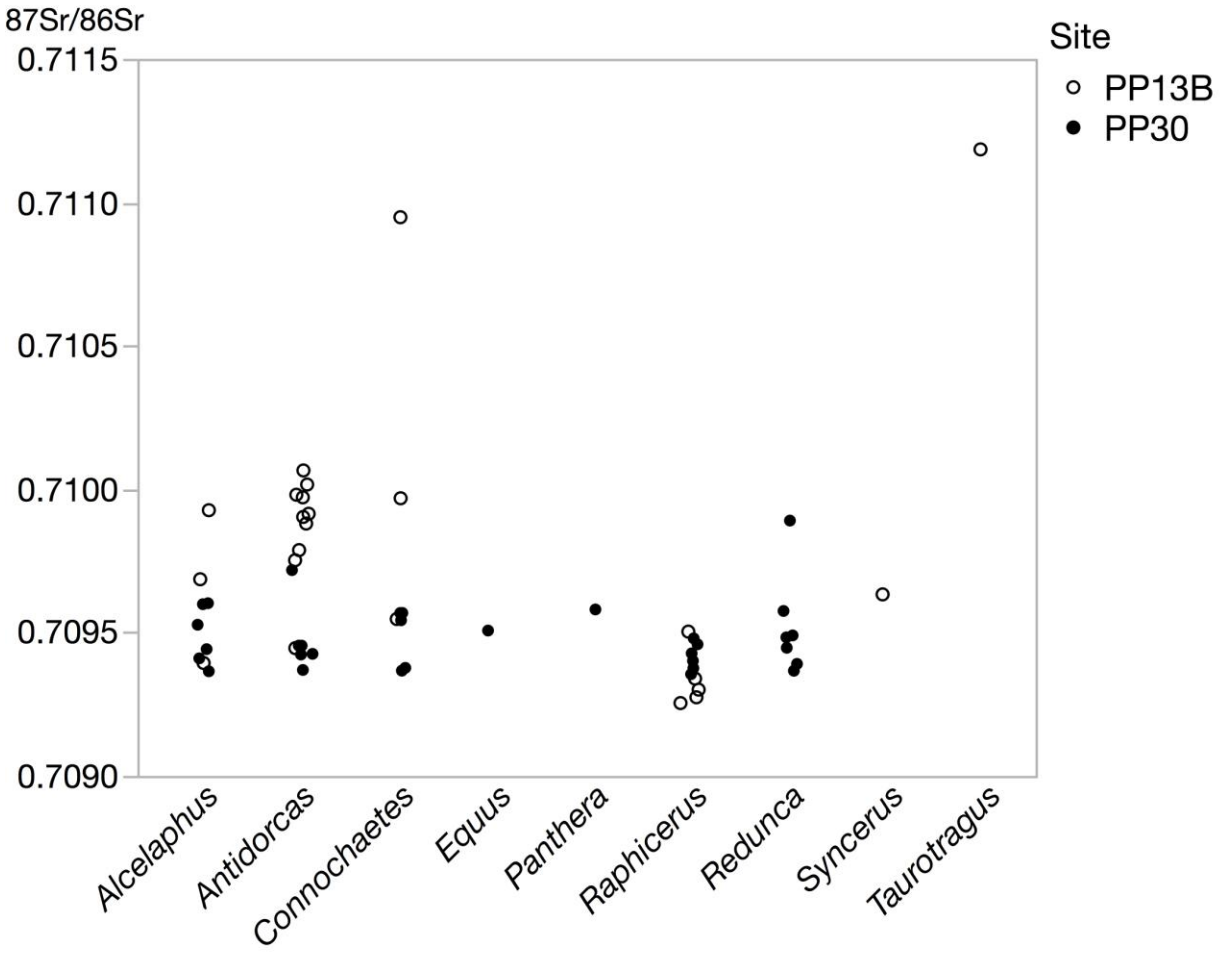

Table 1. List of fossil specimens analyzed from Pinnacle Point sites PP13B and PP30. Stratigraphic position (StratAggregate) and age range for PP13B are based on Marean et al. (2010), and age range for PP30 is from Rector and Reed (2010). For teeth sampled, the term "M1/M2" refers to a single tooth that could be either M1 or M2. Intra- or inter-tooth range of $^{87}Sr/^{86}Sr$ is calculated by subtracting the minimum $^{87}Sr/^{86}Sr$ value from the maximum $^{87}Sr/^{86}Sr$ value of that specimen. MIS Stage = marine isotope stage. Further details for each intra- or inter-tooth sample are available in Table S4.

Taxon	Site	Specimen #	# of intra- or inter-tooth samples	Teeth sampled	$^{87}Sr/^{86}Sr$ (mean of intra- and inter-tooth ± 1σ)	Intra-tooth range of $^{87}Sr/^{86}Sr$	MIS Stage	StratAggregate	Age Range (Ka)
Alcelaphus buselaphus	PP13B	45264	4	M2	0.70939 ± 0.00001	0.00003	5c	DB Sand 3	91-102
		55327	4	M1/M2	0.70993 ± 0.00003	0.00007	5c	Roof Spall-Upper	91-98
		64648	4	M1/M2	0.70969 ± 0.00003	0.00007	5c	Roof Spall-Upper	91-98
	PP30	66613	3	M1/M2	0.70937 ± 0.00001	0.00002	6		151
		66615	3	M1/M2	0.70953 ± 0.00001	0.00001	6		151
		66751	3	M1/M2	0.70941 ± 0.00002	0.00004	6		151
		67209	5	M2, M3	0.70944 ± 0.00001	0.00003	6		151
		67317	3	M1/M2	0.70960 ± 0.00006	0.00012	6		151
		67502	6	M1/M2	0.70960 ± 0.00002	0.00004	6		151
Antidorcas sp. indet.	PP13B	42117	3	M1, M2, M3	0.70998 ± 0.00002	0.00004	5c	Roof Spall-Upper	91-98
		42899	4	M1, M2, M3, P4	0.70988 ± 0.00004	0.00008	5c	Roof Spall-Upper	91-98
		52675	6	M1, M2, M3	0.71002 ± 0.00001	0.00002	5c	Roof Spall-Upper	91-98
		52946	4	M3	0.70991 ± 0.00004	0.00009	5c	Roof Spall-Upper	91-98
		75112	3	M2	0.71007 ± 0.00001	0.00003	5c	Roof Spall-Upper	91-98
Antidorcas marsupialis	PP13B	22316	3	M3	0.70975 ± 0.00003	0.00006	5d	LBG Sand 1	94-134
		34638	4	M3	0.70997 ± 0.00004	0.00009	5c	DB Sand 2	91-102
		42143	3	M3	0.70945 ± 0.00001	0.00002	5c	Roof Spall-Upper	91-98
		51107	4	M1, M2	0.70979 ± 0.00003	0.00006	5c	Roof Spall-Upper	91-98
		80431	3	M1/M2	0.70990 ± 0.00002	0.00003	6	LC-MSA Lower	153-174
	PP30	66377	4	M1, M2, M3	0.70945 ± 0.00003	0.00006	6		151
		66769	4	M3	0.70943 ± 0.00001	0.00002	6		151
		66998	1	M1/M2	0.70972		6		151
		67129	3	M3	0.70942 ± 0.00001	0.00002	6		151
		115358	3	M3	0.70937 ± 0.00001	0.00001	6		151
		115387	2	M1/M2	0.70945 ± 0.00001	0.00002	6		151
Connochaetes gnou	PP13B	41399	4	M1/M2	0.71095 ± 0.00019	0.00046	5c	Roof Spall-Upper	91-98
		52943	4	M3	0.70997 ± 0.00001	0.00003	5c	Roof Spall-Upper	91-98

Taxon	Site	Specimen #	# of intra- or inter-tooth samples	Teeth sampled	$^{87}Sr/^{86}Sr$ (mean of intra- and inter-tooth ± 1σ)	Intra-tooth range of $^{87}Sr/^{86}Sr$	MIS Stage	StratAggregate	Age Range (Ka)
		53188	2	M1/M2	0.70955 ± 0.00001	0.00002	5d	LBG Sand 1	94-134
	PP30	67768	6	M1, M2, M3	0.70937 ± 0.00003	0.00006	6		151
		67867	4	M3	0.70957 ± 0.00001	0.00003	6		151
		115227	5	M3	0.70938 ± 0.00001	0.00003	6		151
		115346	2	M3	0.70957 ± 0.00002	0.00002	6		151
		115433	4	M3	0.70954 ± 0.00001	0.00001	6		151
Equus cf. *quagga*	PP30	67189	3	M3	0.70951 ± 0.00002	0.00003	6		151
Panthera leo	PP30	67374	1	P4	0.70958		6		151
Syncerus antiquus	PP13B	22929	6	M1, M2, M3	0.70963 ± 0.00006	0.00017	5c	DB Sand 2	91-102
Raphicerus campestris	PP13B	64071	1	M1/M2	0.70950		5c	Roof Spall-Upper	91-98
	PP30	66971	1	M1	0.70948		6		151
		67901	2	M3	0.70938 ± 0.00001	0.00001	6		151
		115400	3	M1, M2, M3	0.70943 ± 0.00001	0.00002	6		151
Raphicerus melanotis	PP13B	25575	1	M2	0.70930		3	Truncation Fill	35-39
		28046	1	M3	0.70927		3	Truncation Fill	35-39
		45846	2	M3	0.70934 ± 0.00003	0.00003	3	LB Silt	152-349
		79895	1	M3	0.70925		5d	Roof Spall-Lower	106-114
	PP30	66552	1	M2	0.70940		6		151
		67181	1	M2/M3	0.70946		6		151
		115223	1	M3	0.70935		6		151
Redunca arundinum	PP30	65115	2	M3	0.70937 ± 0.00001	0.00002	6		151
		67035	1	M1/M2	0.70989		6		151
		67278	3	M3	0.70939 ± 0.00002	0.00004	6		151
		67532	2	M1/M2	0.70958 ± 0	0.00000	6		151
		67535	1	M3	0.70948		6		151
Redunca fulvorufula	PP30	66967	1	M1/M2	0.70949		6		151
		67134	2	M1/M2	0.70945 ± 0.00008	0.00011	6		151
Taurotragus oryx	PP13B	26890	3	M1/M2	0.71118 ± 0.00007	0.00013	5d	Roof Spall-Lower	106-114

Table 2. Summary of the fossil animals from PP13B and PP30 sampled for strontium isotope analysis in this study.

Taxon	**Common Name**	**Feeding Classification**	**Propensity to Migrate**	**Number of individuals sampled from PP13B**	**Number of individuals sampled from PP30**
Alcelaphus buselaphus	hartebeest	Grazer	Potentially migratory	3	6
Antidorcas sp. indet.	springbok (indeterminate species)	Grazer	Potentially migratory	5	-
Antidorcas marsupialis	springbok	Browser/Mixed	Potentially migratory	5	6
Connochaetes gnou	black wildebeest	Grazer	Potentially migratory	3	5
Equus cf. *quagga*	zebra	Grazer	Potentially migratory	-	1
Syncerus antiquus	giant buffalo (extinct)	Grazer	Potentially migratory	1	-
Raphicerus campestris	steenbok	Browser/Mixed	Non-migratory	1	3
Raphicerus melanotis	grysbok	Browser/Mixed	Non-migratory	4	3
Redunca arundinum	common reedbuck	Grazer	Non-migratory	-	5
Redunca fulvorufula	mountain reedbuck	Grazer	Non-migratory	-	2
Taurotragus oryx	eland	Browser/Mixed	Potentially migratory	1	-
Panthera leo	lion	Carnivore		-	1

***Highlights (for review)**

Highlights

•Bioavailable $^{87}Sr/^{86}Sr$ near the South African south coast reflects a combination of marine- and bedrock- derived sources that result in a north-south gradient

• Middle and Late Pleistocene ungulates from Pinnacle Point preferred the now-submerged Paleo-Agulhas Plain habitats to those north of the modern coastline

• Pinnacle Point ungulates did not migrate from the coast to the interior (south-north)

• Strontium isotope evidence cannot falsify the hypothesis that large grazers migrated east-west on the Paleo-Agulhas Plain

Supplementary Data

Click here to download Supplementary Data: Supplemental Text Figures S1-S4 Table S1 and S3.docx

Supplementary Excel Tables

Click here to download Supplementary Data: Supplemental Tables S2 S4 S5 S6.xlsx